Review

Assessing the Perspectives of Ground Penetrating Radar for Precision Farming

Federico Lombardi [1,*], Bianca Ortuani [2], Arianna Facchi [2] and Maurizio Lualdi [1]

1 Department of Civil and Environmental Engineering, Politecnico di Milano, Piazza Leonardo da Vinci 32, 20133 Milan, Italy
2 Department of Agricultural and Environmental Sciences–Production, Landscape, Agroenergy, Università degli Studi di Milano, Via Celoria 2, 20133 Milan, Italy
* Correspondence: federico.lombardi@polimi.it

Abstract: The United Nations 2030 Agenda for Sustainable Development highlighted the importance of adopting sustainable agricultural practices to mitigate the threat posed by climate change to food systems around the world, to provide wise water management and to restore degraded lands. At the same time, it suggested the benefits and advantages brought by the use of near-surface geophysical measurements to assist precision farming, in particular providing information on soil variability at both vertical and horizontal scales. Among such survey methodologies, Ground Penetrating Radar has demonstrated its effectiveness in soil characterisation as a consequence of its sensitivity to variations in soil electrical properties and of its additional capability of investigating subsurface stratification. The aim of this contribution is to provide a comprehensive review of the current use of the GPR technique within the domain of precision irrigation, and specifically of its capacity to provide detailed information on the within-field spatial variability of the textural, structural and hydrological soil properties, which are needed to optimize irrigation management, adopting a variable-rate approach to preserve water resources while maintaining or improving crop yields and their quality. For each soil property, the review analyses the commonly adopted operational and data processing approaches, highlighting advantages and limitations.

Keywords: applications of GPR; agricultural geophysics; precision irrigation; soil structural properties; soil hydraulic properties; soil textural properties

1. Introduction

Climate change and population growth exert great pressure on the environment and natural resources. The World Population Prospects [1] estimates that the world population will reach approximately 9.7 billion by 2050, leading to a growing demand for resources and food. In order to face this increasing demand, the Food and Agricultural Organization (FAO) forecasts a more than 50% increase in irrigated food production by 2050 [2]. Given the limited availability of arable land, this food production will determine an agricultural intensification, that means an increasing use of water, fertilizers, pesticides, energy and other inputs. Focussing on water resources, the water imbalance between water supply and demand for agriculture is destined to grow in the coming years, leading to an increase in water scarcity for this sector. Along with this aspect, the rapid urbanisation processes that are currently undergoing in some regions of the world must be taken into account, which are not only affecting how humans consume natural resources, but are also transforming land use [3,4].

In this context, the development and adoption of sustainable production processes are needed to promote an efficient use of natural resources and of water in particular.

Precision Agriculture (PA) is proposed as a solution to achieve a sustainable agriculture. PA is an ensemble of management strategies that, through advanced technologies,

provides tools for a spatially variable and time-variant monitoring, deciding and application of agronomic inputs. The aim of PA is increasing the efficiency in the use of inputs, thus reducing the environmental impacts of agriculture production in order to preserve natural resources for the future. Contemporaneously, the achieved improvement in quality and quantity of crop yields and the cost reduction due to inputs saving should guarantee the economic sustainability of the PA solutions proposed to farmers. Recently, the authors of [5] described PA as the 'use of technologies that integrate sensors, information systems, enhanced machinery, and informed management to improve production by accounting for dynamics within sustainable agricultural systems'.

Specifically, Precision Irrigation (PI) is aimed at reducing irrigation use without creating water stress for crops, by applying water at the *right* time, i.e., only when it is required, with the *right* amount, i.e., depending on the soil water depletion, and at the *right* place, i.e., without creating over-irrigated and under-irrigated areas in the field, thus improving yields [6]. As for water, the variable rate application of the other agronomic inputs (fertilizers, pesticides) leads to a maximization of their use efficiency of use, while reducing their losses in the environment.

The identification of optimum irrigation scheduling must take into account the space–time variability of the soil–crop system, also depending on site-specific agro-meteorological conditions affecting crop water requirements [7]. Therefore, compared to the uniform rate adopted in conventional agriculture, the variable rate and time-variant water application is based on the operators' ability to monitor soil and crop properties and dynamics. In this context, soil and its properties play a fundamental role, because the rooted soil volume constitutes the reservoir from which crop roots extract water for crop development.

Due to the necessity of gathering a deep understanding of soil hydrological behaviour, the last decades have seen a rise of the adoption of remote sensing and geophysical sensors as data sources to support decision-making tools for site-specific irrigation water management. Therefore, geophysical measurements have now become a well-known method for soil investigation at the field scale and farm scales, thanks to their non-invasive, non-destructive, rapid and cost-effective characteristics. Their main advantage is the possibility of investigating agricultural surfaces without disturbing and consequently affecting the soil dynamics [8,9]. In addition, geophysical survey can provide extended insights on both the spatial and the temporal domains, thus offering a bridge between remote sensing observations and point-based measurements. Finally, the retrieved information could also benefit the development of accurate and robust prediction models to analyse soil properties [10–12].

Among one of the many challenges in implementing PI is to obtain an accurate characterisation of the spatial pattern of soil electrical conductivity, a parameter known to be significantly affected by a number of key soil features, including hydrological, structural and textural features [13]. These include, but are not limited to, soil water and organic matter content, soil density and porosity and particle size distribution [14,15]. Complex site-specific behaviours of soil properties affect soil water availability and plant rooting, hence determining crop growth and yield [16–18] Gathering this information has allowed PA to develop from a conceptual idea to a tool for addressing the issue of agricultural sustainability [19,20].

Within the geophysical techniques landscape, Electrical Resistivity (ERT), Electromagnetic Induction (EMI) and Ground Penetrating Radar (GPR) represent the most widely adopted geophysical methods employed for agricultural applications, due to a number of advantages, the main being their high sensitivity to variations in the electrical properties of the soil, i.e., dielectric permittivity and/or electrical conductivity, though providing only an indirect measure of such soil properties. Among them, GPR has been relevantly leveraged in the precision farming domain, as the method is sensitive to both permittivity and conductivity properties, displaying the potential of increasing the collectable information [21,22].

Considering its operating principles, GPR has always shown great promise in scenarios where water content, material porosity and stratigraphic discontinuities represent the predominantly investigated factors, such as in hydrogeological studies, near-surface aquifer delineation, groundwater characterisation and soil hydrology studies. Geological monitoring and surface mining are two additional environments where information on the presence of water and percentage of clay within the stratigraphy acquired through GPR can assist landslide characterisation and the detection of undesired geologic bodies.

GPR is also promising for agricultural applications, where soil moisture, transport and solute issues are of great interest due to their direct impact on crop yield, irrigation management and environmental effects of land usage. In particular, due to GPR's ability to spatially map local soil attributes affecting crop performance, the methodology has been extensively researched and has emerged as possibly the most suitable geophysical technique within the domain.

The present review focuses on the main physico-chemical soil properties relevant for PA procedures, with a particular attention to Precision Irrigation (PI), and on the available advanced geophysical tools to investigate them. In particular, the contribution starts with a detailed analysis of the main soil parameters that directly or indirectly affect the hydrological behaviour of soils, highlighting the research questions that need to be addressed in order to achieve a sustainable water use (Section 2). Then, Section 3 reviews the role that geophysical measurements, in particular Ground Penetrating Radar technique, have played and are playing within the PI domain and the reasons that have secured them a leading role for agricultural soil characterisation. Starting from the core soil parameters previously identified, Section 4 provides a broad review of the different research approaches, methods and processing strategies that have been adopted within the PI domain, highlighting principal characteristics and advantages and limitations. This section, that represents the more relevant contribution of this review, portraits the current landscape of the application of GPR for PI purposes. The paper ends by discussing technological and operational challenges, as well as prospective opportunities related to the use of GPR in soil studies.

2. Physico-Chemical and Hydrological Soil Properties Relevant for PI

Soils are mainly classified on the basis of texture, which refers to the percentage of sand, silt and clay sized particles constituting the mineral fractions of the soil. The soil-type classification based on texture is an important starting point to obtain a first idea of the hydrological behaviour of a soil (i.e., water retention and hydraulic conductivity as a function of the soil water content). However, soil hydraulic properties do not depend only on texture, but also on soil structure and porosity. Indeed, soil structure and porosity in natural conditions are related to textural properties. Soil structure depends on the arrangement of the primary soil particles, creating secondary soil particles (aggregates, clods and pedons) [23]. The formation of these secondary particles depends on the mineralogical composition of soil and on the quality and quantity of soil organic matter. Soils can be classified as structural and non-structural (without aggregates). The latter are mostly coarse and sandy soils with low content of organic matter. Soil structure is a fundamental physical property for agricultural soil, as it is strongly related to the soil porosity (i.e., volume of soil pores over the bulk soil volume, including both soil particles and pores) and pore-size distribution, which play important roles in the hydrological soil processes. The macropores, which are mostly inter-aggregate pores, or even large pore created by dead roots, worms and soil cracks, enable fast infiltration of rain or irrigation water into soil, reducing soil erosion and enabling easier tillage. Conversely, macropores enable fast leaching of nutrients and other solutes, increasing the risk of groundwater pollution. Moreover, macropores enable favourable conditions for aeration and respiration of roots, guaranteeing the soil production functions. Soil organic matter is an important property to ensure the stability of the soil structure, given its resistance against erosion factors such as heavy rains or wind; soils with a high content of organic matter have a stable structure, preserving soil quality [24]. Moreover, soil organic matter increases the soil's ability to retain water by

electrostatic interactions. Soil bulk density, defined as the ratio of the dry weight of soil and its bulk volume (including both soil particles and pores), is an indicator of soil compaction (i.e., reduction in soil porosity). This soil property varies over time (especially in the plugged soil horizon) as a result of agricultural soil management and interactions with agro-meteorological factors. Although rarely measured, soil compaction is an important property of agricultural soils due to its variability over time, connected to soil degradation. Indeed, the reduction in soil porosity and, thus, in bulk density plays a critical role for water and solute transport processes in agricultural soils, as it determines decrease in soil hydraulic conductivity [25], which affects irrigation water infiltration and nutrient uptake, thus increasing runoff and soil erosion [26–29]. Moreover, soil porosity and bulk density are strongly related to soil structure: as already introduced, a well-developed and stable soil structure is fundamental for productive soils [30,31].

Soil texture, structure and its organic content greatly affect the soil water retention properties due to the interactions between water contained in the pores and the solid phase. The volumetric Soil Water Content (SWC) expresses the relative quantity of water in the soil, as the ratio of water contained in the soil pores and the bulk soil volume [32]; its value is maximum at saturation, when the pore system is completely filled with water. Soil Matric Potential (SMP) expresses the tension of water in the pore system, which is negative due to the attraction between water and the solid phase, becoming null at soil water saturation. The relationship between SMP and SWC is described by the Soil Water Retention Curve (SWRC). The SWRC is typical of a specific soil, and depends on its texture, structure and soil organic matter. The soil–water constants are specific points on the SWRC, with SWCs (or SMPs) corresponding to different levels of water availability to plants. The soil–water constants often used in the irrigation management are Field Capacity (FC), Point of Limited Availability (PLA) and Wilting Point (WP). FC is the maximum SWC (and SMP) available for plants after the drainage of water present in the larger pores following a rain or irrigation (i.e., water content between saturation and FC is not available for plants); PLA is the SWC (and SWP) at which the actual crop transpiration rate starts to be lower than its potential rate, thus leading to a decrease in biomass production. WP is the SWC (and SMP) at which the crop transpiration stops since crops are not able to counteract the tension with which water is retained at the solid matrix (after reaching this point, no further irrigation is effective). Furthermore, Available Water Capacity (AWC) is the range of SWC available to plants in the soil root depth, from WP to FC.

Soil hydraulic conductivity also depends on SWC (and, thus, on SMP), which is a fundamental soil variable to determine the water flow rate in soils. Again, the relationship between SWC (and SMP) and soil hydraulic conductivity is soil dependent. Particularly, saturated hydraulic conductivity (i.e., hydraulic conductivity at saturation) is expected to be higher in coarse soils than in fine soils, but the unsaturated hydraulic conductivity depends mainly on soil texture, structure and organic matter content, as well as on the agronomic operations conducted. Indeed, these factors affect porosity and pore size classes. The presence of skeleton (rock fragments or cobbles with a dimension > 2 mm) in soils deserves a separate discussion, since it modifies the volume available for water in the soil, as well as the soil hydraulic conductivity.

The knowledge of soil hydrological behaviour, that means soil water retention and hydraulic conductivity curves (as a function of SWC/SWP), allows for the accurate description of water flows in agricultural soils by using physical-based agro-hydrological models involving the solution of the Richards' equation. Through these approaches, it is possible to support the irrigation management and planning at different spatial scales. However, measurements of soil water retention and hydraulic conductivity curves in field or laboratory are very expensive in term of time and economic costs; additionally, they concern single points in soil profiles and are consequently not applicable in real agricultural production systems. As a matter of fact, the hydrological properties of soils vary not only in the horizontal dimensions, but also along the vertical dimension, since soils are generally characterized by an alternation of horizons with different characteristics.

To overcome this fact, soil hydrologists and irrigation specialists very often describe the soil water retention and hydraulic conductivity curves through analytical models (e.g., Brooks and Corey [33], Van Genuchten [34]), and derive their parameters by the knowledge of fundamental soil properties (texture, soil organic matter and, if available, bulk density, porosity, structure, FC and WP), which are more easily measurable and often quantitatively described (at least texture and organic matter content) in the soil profiles associated with regional/national soil maps. These soil properties are inputs for empirical models called Pedo-Transfer Functions (PTFs), which are used to estimate parameters included in the analytical models describing the soil water retention and hydraulic conductivity curves [35–37]. In particular, PTFs are generally statistical regression models developed on the basis of large datasets including several hundred measurements of coupled physico-chemical and hydrological soil parameters.

2.1. Reference Values for Physico-Chemical and Hydrological Soil Properties

The range of variability of the main soil properties can be deduced from the wide datasets collected to develop the different PTFs. The USDA Soil Survey Manual [38] refers to the work of [39] to describe the variability of the saturated hydraulic conductivity for the USDA soil texture classes, based on bulk density and particle size distribution (percentage of sand, silt and clay). The authors of [40] illustrate the soil properties variability based on measurements of 1323 soils in the USA. More recently, a review work in 2016 [41] reports the main research that developed PTFs worldwide: based on the largest datasets, the authors of [39,40,42–45] developed PTFs for soils in the USA (5320 soil samples), while the authors of [46] developed PTFs for soils in Europe (HYPRES database, 4030 soil samples). Additionally, the authors of [47,48] developed PTFs by the neural model ROSETTA, based on a dataset of 2134 soil samples collected in North America and Europe.

Table 1 shows the variability of the soil properties (sketched in Figure 1) relevant for PI, based on the aforementioned datasets. Totally, the dataset considered in [39,40,42] mostly covered the agricultural soils characterised in [49]. Sand, silt and clay contents were shown to range, respectively, from 0.1 to 99% (mean 56%), from 0.1 to 93% (mean 26%) and from 0.1 to 94% (mean 18%); organic matter content ranged from 0.1 to 12.5% (mean 0.66%), and bulk density from 0.6 to 2.09 g/cm^3 (mean 1.42 g/cm^3). Soils used for the ROSETTA PTFs were characterised by mean values of porosity and saturated hydraulic conductivity equal to 0.411 cm^3/cm^3 and 5.04 cm/h, respectively.
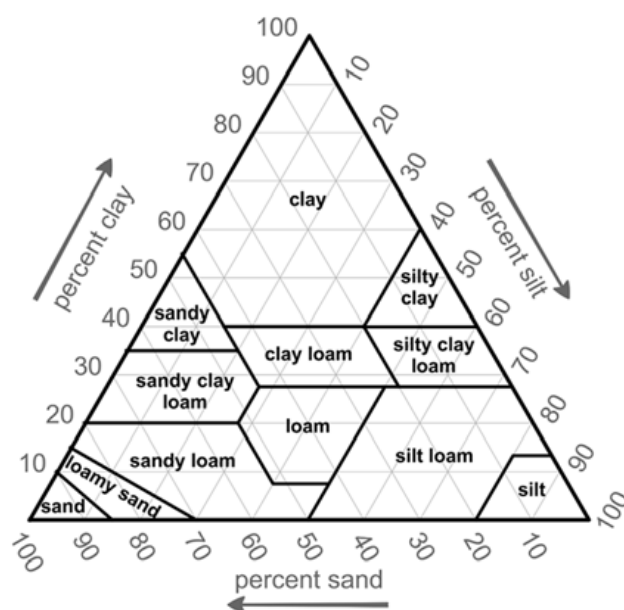

Figure 1. Soil textural triangle, as defined by the USDA. Derived from [38].

Table 1. Soil hydraulic properties variability for the USDA texture classes. Mean values are reported for each textural class, and ±1 standard deviation values are in brackets.

| USDA Texture Class | Sample Size | [39,40] | | | | Sample Size | [43] | Sample Size | [47] | |
		n (cm³/cm³) [1]	FC (cm³/cm³) [2]	WP (cm³/cm³) [3]	Ksat (cm/h) [4]		OM (%) [5]		n^* (cm³/cm³) [6]	Ksat (cm/h) [4]
Sand	762	0.437 (0.374–0.500)	0.091 (0.018–0.164)	0.033 (0.007–0.059)	21.00	660	0.71 (SD 1.06)	308	0.375 (0.320–0.430)	26.78
Loamy Sand	338	0.437 (0.368–0.506)	0.125 (0.060–0.190)	0.055 (0.019–0.091)	6.11	198	0.61 (SD 1.16)	201	0.390 (0.320–0.460)	4.38
Sandy Loam	666	0.453 (0.351–0.555)	0.207 (0.126–0.288)	0.095 (0.031–0.159)	2.59	371	0.71 (SD 1.29)	476	0.387 (0.302–0.472)	1.60
Loam	383	0.463 (0.375–0.551)	0.270 (0.195–0.345)	0.117 (0.069–0.165)	0.68	203	0.52 (SD 0.99)	242	0.399 (0.301–0.497)	0.50
Silt Loam	1206	0.501 (0.420–0.582)	0.330 (0.258–0.402)	0.133 (0.078–0.188)	1.32	497	0.58 (SD 1.29)	330	0.439 (0.346–0.532)	0.76
Silt	-	-	-	-	-	-	-	6	0.489 (0.411–0.567)	1.82
Sandy Clay Loam	498	0.398 (0.332–0.464)	0.255 (0.186–0.324)	0.148 (0.085–0.211)	0.43	250	0.19 (SD 0.34)	87	0.384 (0.323–0.445)	0.55
Clay Loam	366	0.464 (0.409–0.519)	0.318 (0.250–0.386)	0.197 (0.115–0.279)	0.23	175	0.10 (SD 0.51)	140	0.442 (0.363–0.521)	0.34
Silty Clay Loam	689	0.471 (0.418–0.524)	0.366 (0.304–0.428)	0.208 (0.138–0.278)	0.15	209	0.13 (SD 0.42)	172	0.482 (0.396–0.568)	0.46
Sandy Clay	45	0.430 (0.370–0.490)	0.339 (0.245–0.433)	0.239 (0.162–0.316)	0.12	61	0.38 (SD 1.20)	11	0.385 (0.339–0.431)	0.47
Silty Clay	127	0.479 (0.425–0.533)	0.387 (0.332–0.442)	0.250 (0.193–0.307)	0.09	-	-	28	0.481 (0.401–0.561)	0.40
Clay	291	0.475 (0.427–0.523)	0.396 (0.326–0.466)	0.272 (0.208–0.336)	0.06	72	0.38 (SD 0.83)	84	0.459 (0.380–0.538)	0.61

[1] Porosity; [2] Field Capacity (evaluated as SWC at—33 KPa); [3] Wilting Point (evaluated as SWC at—1500 KPa); [4] saturated hydraulic conductivity; [5] organic matter; [6] porosity (evaluated as SWC at saturation).

2.2. Soil Characterization and Mapping

In order to apply PI, the within-field soil variability must be accurately described. According to the traditional approach in soil detection, a higher accuracy in soil mapping requires us to increase the number of sampling points. Undisturbed soil samples are taken at different soil depths by means of an auger; samples are used for the determination of soil texture and organic carbon. Undisturbed soil samples for the quantification of bulk density and water retention and hydraulic conductivity properties require the opening of trenches to directly collect soil in metal samplers to preserve soil structure. Consequently, the achievement of a detailed description of soil variability at the field scale through a traditional soil survey is very expensive and time consuming, since a dense sampling network should be designed and applied. Innovative approaches introduced in the 1990s adopt geophysical sensors to quantify soil properties through quick and non-invasive surveys (i.e., soil proximal sensing).

3. Agricultural Geophysics and Ground Penetrating Radar

From what has been previously described, it is evident the key role that the knowledge of the electrical properties of soil plays in precision farming processes and decisions [50,51]. Soil physical properties, such as texture, structure, porosity and density, hydrologic attributes, including SWC, and chemical features, are known to relevantly affect the electromagnetic properties of agricultural soils [52,53].

The soil properties mainly affecting EC are SWC, texture (particularly clay content) and bulk density [16–18]. Other factors influencing EC are soil temperature and compo-

sition of soil solution. As matter of fact, EC depends on the free electrical charges either carried by dissolved ions (i.e., volume conduction), or carried by the solid/liquid interfaces (i.e., surface conduction). As volume conduction dominates in soils, EC is very sensitive to SWC and to the composition of the soil solution. The relationship between EC and SWC is described by Archie's law; nevertheless, in the range of variation of SWC for environmental and agronomic applications, that relationship is quasi-linear [54]. The influence of soil solution composition is more important when the soil is saturated, while it can be neglected for unsaturated soils. Moreover, for salt soil or sodic soil, EC increases linearly with the increasing electrical conductivity of the soil solution [55]; otherwise, the composition of the soil solution can be neglected if the geophysical survey is carried out sufficiently far from the fertilization periods.

The surface conduction depends on the nature of soil particles and its effect on EC is not negligible in soils containing clay [56]; organic matter content also affects EC [57]. Time-lapse EC surveys on the same site allow us to detect variations of bulk density; indeed, under dry conditions, increasing porosity due to cracking, perforation by worms or roots or tillage operations causes lower EC, while reduction in porosity due to soil compaction determines higher EC [58]. Porosity is a dominant factor on EC under very dry soil conditions, as the EC value for air is very low; in this case, spatial variability in EC detection is mainly due to variations in bulk density. However, for soils with low porosity and under dry conditions, variations in EC discriminate soils with different textures. Conversely, under wet soil conditions, EC is sensitive mostly to SWC, then differences due to texture or other factors are hardly detectable. Finally, the presence of areas with soil compaction are more easily detected through EC survey under dry soil conditions.

It is important to consider the temperature effect for time-lapse EC surveys, particularly in the first 20 cm of soil depth, as temperature can variate a lot during the day, especially in summer. In these cases, EC must be assessed at the reference temperature usually equal to 25 °C by applying a correction equation [59].

Concerning dielectric permittivity, it is highly correlated to SWC [60,61], as dielectric permittivity for water is much higher than that for other soil constituents; indeed, the relative dielectric permittivity of air is 1, while it is 80 for water, and 3–8 for dry mineral materials (with air in pore spaces); hence, the addition of water in the soil pores drastically increases the dielectric permittivity of soil. Soil texture, organic matter content, porosity and temperature affect soil dielectric permittivity as well, even though these factors are usually negligible as their effects are secondary compared to the effect of water. The relationship between SWC and soil dielectric permittivity is described by empirical models, as Topp's model calibrated for soils with different textures. Under completely dry soil conditions, mapping dielectric permittivity provides information on the spatial variability of porosity and soil mineralogy [62–64]; moreover, the vertical variability of the dielectric permittivity allows us to describe soil layering.

The geophysical methods predominantly used for agricultural purposes are ERT, EMI and GPR; additional methodologies, such as magnetometry, self-potential and active seismic methods, have the potential for substantial future use in agriculture, but at present are being limitedly employed for agricultural purposes [21,65,66].

In agriculture applications, the importance of measuring the electrical properties of soils dates back to the end of nineteenth century [67–69], with the first electrical prospection experiments being performed by Conrad Schlumberger in France in 1912 [70,71] and Frank Wenner in the United States in 1916 [72]. The earliest application was to determine the soil water content, while advancements have shifted towards the measurements of soil salinity [73,74], which can be considered the beginning of the agricultural geophysics research branch. ERT methods (Figure 2) are based on the measurement of the soil resistance to current flow across (typically) four electrodes inserted along a line on the soil surface at a specified distance. Despite its wide adoption within the field, mainly due to the simplicity in converting sensor measurements to EC values and the possibility of repeated measurements over time, the technique cannot be considered strictly non-invasive, as it

requires good contact between the soil and the electrodes and the non-uniqueness of the inversion schemes, hence limiting its applicability and measurement reliability [56].

Figure 2. ERT prospection for precision farming. (**a**) Example of ERT on-the-go sensor [57]. (**b**) Example of ERT result showing the shallow conductivity map for an agricultural field (black to white colour scale, low to high values).

The use of EMI dates back to the late 1970s, and particularly to 1976, when the first EMI sensor was patented [75] with the main purpose of assessing soil salinity features as a response of the growing need for information on soil properties and behaviour [76,77]. EMI sensors typically transmit a primary EM field inducing electrical currents in the soil, and a receiver records the secondary field, which is used to estimate the EC values. The first reported use of such technique in 1979 highlighted the suitability of the methodology in providing fast and continuous measurements due to its non-invasive configuration, though at the same time stressing the limited depth information that can be gathered [78]. Principal evolution of the technique encompassed the estimation of EC through the development of site-specific empirical relationships for inverting both low conductivity media and higher conductivity values, i.e., when the linearity assumption between the quadrature component of the received EM field and the measured EC does not hold anymore [79–81].

ERT and EMI on-the-go sensors (Figures 2a and 3a) are mainly employed in soil survey at the field scale for PA applications. These sensors measure the soil electrical conductivity (EC) at different depths, which is related to both physical and chemical properties of the soil profiles. Since the latter are relevant conditions known to adopt a variable rate management of irrigation and fertilization, according to PA practices, high resolution EC maps (Figure 3b), quite easily obtained through geophysical sensors, are used to delineate the different homogeneous Management Zones (MZ) within the field [82–84], where soil variability is expected to be less than among MZs. As a matter of fact, the delineation of MZs can be used to design a soil sampling network with a limited number of points, optimally located within each MZ and distributed among the MZs, thanks to the soil variability scouting provided by the EC maps. In each sampling point, soil water retention and hydraulic conductivity properties can be directly measured on undisturbed soil samples collected at different depths, or otherwise indirectly evaluated from texture data measured on disturbed soil samples. These measures allow us to characterize the soil in each MZ as well as to derive maps for specific soil properties through calibrating empirical models [83,85–92].

(**a**)

(**b**)

Figure 3. EMI prospection for precision farming. (**a**) Mobile platform for EMI survey [79]. (**b**) Example of soil apparent EC map obtained with EMI sensor over a vineyard (red to blue colour scale) [85].

The accuracy in soil mapping for specific properties depends on their relationship with EC measurements, as well as on the ability of the geophysical survey to describe the soil variability in both horizontal and vertical directions.

Magnetometers measure anomalies in the strength of the Earth's magnetic field due to subsurface magnetic heterogeneities, including soil iron content and drainage pipes [93,94]. Instead, seismic methods are based on the analysis of the propagation of elastic waves into the ground, thus measuring density and elastic property anomalies; from laboratory studies, it has been shown that wavelet characteristics (velocity and amplitude) can be correlated with soil compaction, porosity, bulk density and soil water content [95–97]. Finally, the self-potential method, one of the few passive geophysical techniques within the domain, records the naturally occurring electric potential difference between two locations; such measurements are associated with electrokinetic processes generated by leakages, water flows, water table depression and horizontal spatial patterns for soil salinity and soil clay content [98,99].

Along with the emerging trend in sensor development for agricultural applications, the decade between 1970 and 1980 has seen the consistent introduction of GPR as a tool to study the variability of soils [100–102]. The GPR technique utilises high frequency EM wave reflections at boundaries between materials exhibiting discontinuity with different electrical properties to produce a continuous vertical profile of the investigated area in a cross-section along a transect. GPR is an electromagnetic method similar in principle to the seismic reflection technique, except that it is based on the propagation and reflection of electromagnetic waves rather than acoustic ones. Essentially, a transmitter antenna radiates an electromagnetic wave that propagates into a lossy dielectric material until it encounters a change in material properties, represented by a contrast in the electromagnetic impedance feature. At this interface, a part of the wave is scattered back, and its reflection is recorded by the receiving equipment. The other portion of the wave might instead be transmitted and, therefore, it will continue to propagate. The magnitude of the reflection and transmission phenomena depends on the sharpness of the contrast, as well as on the physical and geometrical features of the discontinuity structure. The amplitudes of the received echoes and the corresponding arrival times are then processed to determine characteristics, nature and location of the discontinuity.

A standard GPR system (Figure 4) consists of a signal generator, a separate transmitter and receiver antennas, typically housed in a single case, and a portable laptop for real-time data display and further data processing. According to the signal generation system, GPR

systems are classified into time domain and frequency domain radar, the first category being the most widely adopted in commercial systems. An additional distinction is made depending on whether the equipment is working in contact with the surface (ground-coupled) or above it (air-launched). The choice of one or the other approach represents a trade-off between survey logistics and data interpretability.
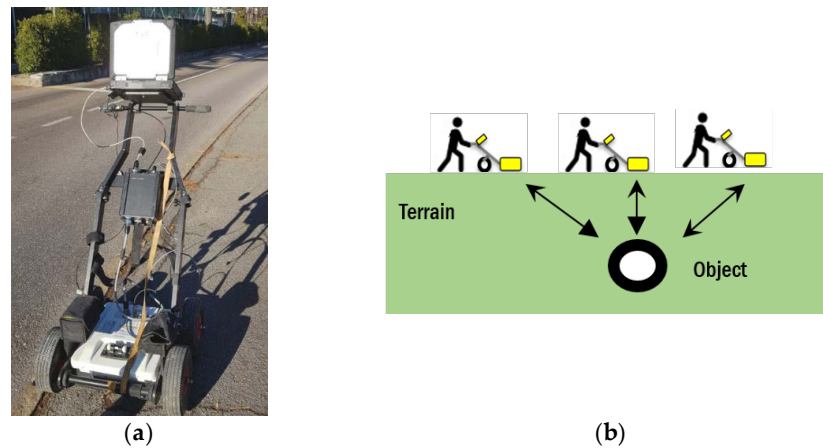

(**a**)　　　　　　　　　　　　　　　　　　(**b**)

Figure 4. GPR prospecting system. (**a**) GPR components. (**b**) Sketch of survey modality.

The first reported feasibility study was performed in 1979 in a joint effort by NASA, USDA-SCS and the Florida Department of Transportation [103,104]. The main outcome of such a study was that the penetration performance of the methodology was not consistent throughout all the US states (Figure 5), suggesting a distinct dependency with local soil properties and, therefore, the suitability of the GPR methodology for estimating variations in soil properties to classify soils and develop taxonomic composition of soil units, as for example the USDA-NRCS soil suitability map [105–107]. In particular, what emerged was the sensitivity of GPR to detect abrupt changes in physical properties, such as texture and bulk density, and in SWC and chemical properties, including organic matter and minerals. Subsequent analysis and studies have demonstrated a decrease in cost (reported 70%) and an increase in survey efficiency (reported 210%) comparing GPR profiling against alternative transect techniques [108].
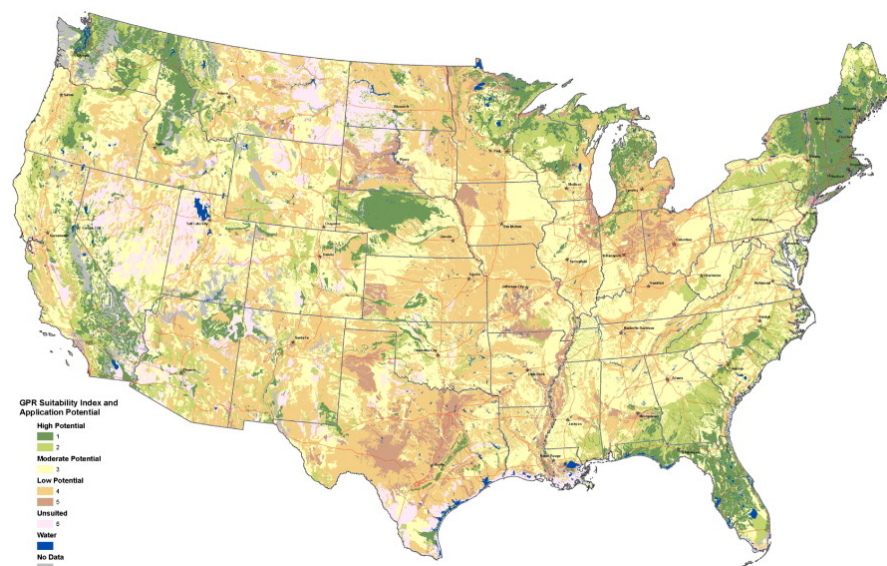

Figure 5. Soil suitability classification as inferred from GPR measurements, from green (high potential) to light red (unsuitable). Derived from [107].

At the earliest stages, GPR technology was adopted to determine organic layer thickness and depth of stratigraphic discontinuities [109,110], to identify and classify soil types [111] and to detect hard pans [112]. In addition, the effectiveness of GPR in providing time-lapse monitoring of water movements and water table depth variations [113,114], and in identifying preferential flow paths and moisture-front movements [115–117] became evident.

Table 2 summarises the main features of each geophysical methodology.

Table 2. The main features of geophysical methodologies.

Geophysical Method	Physical Property	Potential Application
Resistivity	Electrical resistivity	Soil drainage Soil salinity Spatial variation Soil water content
Electromagnetic induction	Electrical conductivity	Clay-pan depth Soil nutrient Soil salinity Spatial variations Soil water content
GPR	Dielectric constant and electrical conductivity	Soil classification Vertical microvariability Bedrock depth Plant root biomass Flow pathways Drainage pipes
Magnetometry	Magnetic susceptibility	Drainage pipes Soil pollution and iron content
Self-potential	Electric potential gradient	Soil salinity Soil water content
Seismic	Density and elastic moduli	Soil compaction Soil porosity

Ground Penetrating Radar Application for PA

Even from these early studies, a number of clear advantages of the GPR methodology emerged: (1) the capability of providing large quantities of continuous, high-resolution subsurface data, (2) the possibility of jointly estimating the geometrical and the geophysical characteristics of the site, (3) a completely non-destructive and potentially non-contact operation, and as a consequence of that, (4) improved speed of investigation. All these features have gained GPR technology a wide recognition within several application areas, from engineering to hydrogeology, archaeology and forensics [118–120]. Successful application of GPR has been reported for subsurface heterogeneities characterisation, as well as for delineating complex subsurface geometries [121].

What can be considered an added value that GPR has brought into the agricultural domain is its sensitivity to both the properties which characterize the electrical behaviour of soils, i.e., the dielectric permittivity and the electrical conductivity. The combined estimation of these two properties by GPR measurements allow for a more detailed soil characterization [122–125]. Through GPR detection, soils are fundamentally described in terms of their electrical properties, i.e., permittivity and electrical conductivity values, and in terms of some coefficients describing the rates of change of those properties with temperature, density, composition and stratigraphy. Such attributes determine how soils react to an electric field and are inherently related to soil physical properties and, therefore, to its constituents [126]. In particular, soil dielectric permittivity is mostly dominated by soil porosity, water saturation and texture [127–129], as a consequence of the large contrast in the dielectric values of air and water. Moreover, simultaneous measurements of soil electrical conductivity allow for the evaluation of the type of fluid contained within the

pore-space (and its chemical composition), as well as the soil mineralogy and the clay content [130–132].

In addition, a strong relationship has been well documented between soil permittivity, SWC and phase velocity, while the same direct effect does not exist with power attenuation [133,134]. Since the soil dielectric constant is one of the key factors governing wave propagation, reflection and scattering phenomena, GPR measurements are clearly a reliable and accurate way to estimate such attributes [135]. Finally, it should be also mentioned that a number of materials, including water and clay, exhibit a frequency-dependent impact on dielectric permittivity. This means that analysing the spectrum of the received signal, in addition to its amplitude, can provide a further tool to determine the presence of specific constituents and better characterise soil type [136–139].

Table 3 describes the electrical conductivity and the relative permittivity values for different materials and soils [140].

Table 3. Typical range of electrical characteristics of different materials.

Material		Conductivity S/m	Relative Permittivity
Air		0	1
Water	Fresh	1×10^{-5}	81
	Sea	1×10^{3}	
Sand	Dry	1×10^{-6}	4
	Wet	1×10^{-2}	20
Clay	Dry	1×10^{-2}	4
	Wet	1	25
Limestone	Dry	1×10^{-8}	7
	Wet	1×10^{-3}	8
Soil sandy	Dry	1×10^{-4}	7
	Wet	1×10^{-2}	20
Soil loamy	Dry	1×10^{-4}	7
	Wet	1×10^{-2}	20
Soil clayey	Dry	1×10^{-2}	7
	Wet	1	20

From those values, two main considerations emerge. Firstly, comparing the dry/wet characteristics, it is evident how the presence of water impacts both the electrical properties of the material. While a major increase is experienced by the permittivity, variations are also evident in the conductivity values (e.g., dry and wet clay). Salinity, instead, severely affects the conductivity only, leaving the dielectric features almost unchanged (e.g., fresh and sea water) [141].

The feasibility of a GPR investigation, and, thus, its suitability, is primarily determined by (1) the existence and the strength of an EM impedance contrast on sides of the interfaces between different materials, (2) material attenuation and (3) the resolution performance within the depth of interest.

The magnitude of the impedance contrast defines the amplitude of the reflected wave [142,143], thus effectively affecting the possibility to have a record from specific subsurface materials (on each side of the interface), and it is directly related to the ratio between the dielectric constant of those materials [144]. The reflection amplitude of the GPR signal increases for water-saturated soils and for high levels of salinity and clay content. Therefore, since the effect of saturation on the relative permittivity is dominant, the reflection amplitude could give an estimate of the SWC of the underlying soil layer [145–147].

Material attenuation controls the wave amplitude loss during propagation, hence determining the maximum achievable penetration depth [148]. Attenuation is directly dependent on both permittivity and conductivity; hence, it is highly sensitive to SWC,

clay and chemicals [149–151]. The attenuation is also linearly dependent to the operating frequency; therefore, the higher the frequency, the more pronounced will be the attenuation and the achievable penetration will be reduced [152,153]. Additionally, the attenuation of GPR energy shifts the amplitude spectrum of the radar pulse to lower frequencies, known as absorption [154–156].

Theoretically, resolution is generally defined as the capability to distinguish, in time and space, two events that are close to each other and it determines to what extent the GPR system is capable of delineating thin layers of heterogeneous soil [157–159]. The value is mainly governed by the propagating wavelength and the reflection depth, implying that a wave propagating in different materials exhibits different resolution performance [160,161], and that, despite typically considered a constant value, resolution performance will degrade with depth due to the absorption effect which limits the high frequency content of the propagating wave [162,163].

Finally, though it is not possible to accurately determine GPR performance in terms of maximum penetration, since it depends also on radar-system-dependent parameters and ground- and target-dependent ones, the combined effect with attenuation allows us to recognize different soil conditions [163,164]. Indeed, wet soils quickly attenuate radar signals and, hence, significantly limit the penetration depth (high conductivity, high permittivity), at the same time allowing us to appreciate finer details and features (low velocity and short wavelength). As a final consideration, the high spatial and temporal resolution achievable allows us to cope with the variability of the measured physical properties over very short horizontal and vertical distances. This GPR performance in spatial resolution is an important feature for application in the PA domain, bearing in mind that the soil thickness of interest in agricultural geophysics is within a 2 metre zone directly beneath the ground surface [165,166].

4. Review of GPR Applications to Soil Properties Estimation

The majority of the soil parameters described in Section 2 relies upon the arrangement of solid particles and voids in the soil, as well as from the presence in the void space of water or other fluids. Hence, their determination has been typically accomplished by exploiting relative changes in the soil dielectric constant that caused the reflections and EM wave velocity. In any event, the choice of the optimal survey approach depends on the specific purpose and site condition. Many successful experiments exploited reflection coefficients and early-time signal characteristics to develop site-specific relationships between amplitude attributes and shallow-soil permittivity. This applies not only for the soil hydraulic properties, which can very often be considered the final information to be gathered, but also for the estimation of the physical soil properties, such as soil porosity, compaction and structure.

Inferring specific quantities or constituents, such as soil wilting point and organic matter content, and determining hydrodynamic parameters, including water retention characteristics, has been so far accomplished in a semi-quantitative manner. This mainly includes the development of numerical models of GPR signals and electromagnetic field propagation to explore the relationships between specific subsurface properties and GPR data, and inversion schemes to iteratively reconstruct the true geometrical and amplitude data from the reflections picked from the GPR data. These partial achievements are due to the fact that their quantitative definition by interpreting GPR profiles alone is still not feasible, and that some of the most widely used models relating dielectric constant to the soil constituents are purely empirical.

After a brief description of the currently available GPR technology and the most successful acquisition strategies, this section provides a comprehensive review of the different research approaches, methods and processing strategies that have been adopted for soil characterization within this research domain, highlighting principal characteristics, advantages and limitations. Four main topics will be covered: the determination of the soil textural properties and of the main soil constituents, the estimation of the attributes defining

the soil structural properties and the characterisation of the soil hydraulic properties. Despite not strictly being a soil property but a time-varying soil condition, the first subsection focusses on the review of the SWC estimation techniques. This inclusion has been deemed necessary due to the fact that it represents the starting point wherefrom the aforementioned soil properties are consequentially estimated.

4.1. GPR Equipment Characteristics and Survey Strategies

To derive the most from a GPR survey, key issues to be considered include subsurface structure characteristics, GPR antenna selection and survey design.

From what has been previously described, the two main requirements for a successful GPR survey for agricultural applications are the capability of penetrating down to the first metre below the surface and a centimetre-scale resolution to adequately characterise the specific soil property. For these reasons, the majority of the GPR equipment adopted for agricultural investigations exhibits an operating frequency ranging from approximately 200 MHz to 900 MHz, corresponding to a vertical resolution (calculated as a quarter of the wavelength) of 3 to 14 cm for dry soils, and of 8 to 18 cm for wet soils, thus making the GPR technique the geophysical proximal sensing method with arguably the highest spatial resolution in describing vertical soil profiles. Concerning penetration, lowering the frequencies will ensure a proper performance even in less favourable soil conditions (e.g., clay material).

Regarding the system architecture, time domain or pulsed radars constitutes the majority of commercially available GPR devices due to the ease of engineering, limited cost and fast data acquisition. On the contrary, the principal advantages of frequency domain radar are a larger frequency bandwidth, a wider dynamic range and the possibility of shaping the power spectral density. Optimising the frequency range means that the system operational parameters can be optimised depending on the survey scenario: energy at high frequency is saved if the soil exhibits high attenuation, at the same time maintaining sufficient resolution performance. Until recently, the time-consuming calculations associated with the frequency domain data inversion limited its application, but due to continuously increasing computational capabilities, this limitation no longer applies.

Typical GPR survey collects transects along a single, fixed direction by deploying a single transmitter and receiver pair moving together over the surface and maintaining the same mutual distance. This architecture is the most commonly adopted approach, as this allows for relatively fast and operationally straightforward data acquisition. Alternatively, a multi-static survey geometry, in which the transmitter and the receiver are independently managed and moved, can be adopted. These strategies have been extensively employed for the characterisation of soil velocity, particularly for the reconstruction of vertical and lateral distributions, as they could provide an accurate and precise estimate, and to reduce random and non-coherent disturbances. However, such choice is clearly more time-consuming and more complex to implement.

Operationally, equipment should be able to survey rugged topography and unfavourable terrain conditions, as well as allow the efficient execution of a large number of profiles. These requirements have greatly benefitted from one of the major GPR advancements of the last few years, that is the implementation of a multichannel (i.e., array) air-launched GPR system. Such devices have not only allowed for the simultaneous acquisition of multiple GPR profiles, spatially consistent and highly correlated, but the possibility of mounting the antennas on a vehicle has enabled operationally suitable stand-off distances and the rapid survey of wide areas (Figure 6).

(**a**)

(**b**)

Figure 6. Example of state-of-the-art GPR equipment for precision agriculture. (**a**) Vehicle mounted air-launched GPR array. (**b**) Vehicle mounted ground-coupled GPR array.

4.2. Soil Water Content

Among the reviewed studies, applications to determine SWC are by far the most frequent [167–169], probably as a consequence of the fact that detecting soil moisture levels represent a task which spans several domains, including engineering and other environmental applications [170,171] (Figure 7a).

As the presence of water predominantly affects the dielectric permittivity of the soil, a feature that has gained GPR an advantage over both ERT and EMI [172,173], one of the most adopted approaches is the analysis of GPR wave velocity via reflection data [174–181]. It works by first converting the EM wave velocity into soil dielectric permittivity by inverting the measured travel time, and then translating it into a volumetric water content through an empirical relationship [61,182,183].

To properly assess the EM wave velocity, the depth of the reflector should be known. Consequently, information on the subsurface velocity at certain locations are obtained by varying the spacing between the transmitter and the receiver. These multi-offset configurations, known as common source, common receiver and common mid-point schemes, additionally permit us to estimate the ground wave amplitude and frequency attributes [184–190] (Figure 7b). Such an acquisition strategy allows for the simultaneous determination of the reflector depth and the wave velocity; hence, it is much more suitable to estimate SWC, but the price to pay is a more complex system design and a labour-intensive acquisition [191]. Another strategy is cross-borehole radar tomography, both vertical and horizontal, a method that provides higher resolution insights into the subsurface, but is limited in the maximum lateral extent that it can afford [192–196]. It can, therefore, be inferred that these two approaches are most suitable for small-scale investigation or numerical model calibration.

Research efforts have also been focussed on detecting and quantifying changes in SWC through time-lapse investigations, an approach considered to be a valuable strategy to monitor subsurface hydrological processes. Time-lapse GPR has demonstrated its capability in resolving small size features even in challenging surroundings where many reflectors are present [197–201]. The method works through a differencing approach by interpreting changes in travel time between reflection horizons or sample-to-sample variations. This aspect represents the main advantage of the methodology: being based on a change-detection approach limits the potential bias introduced by the choice of the specific dielectric mixing model (e.g., Topp's, Archie's or suitable alternatives), a mandatory requirement when the aim is to provide an absolute estimate of the investigated feature. Instead, the main prerequisite to ensure the correctness of the differencing scheme is the fact that highly reproducible data are necessary; hence, data consistency (including measurements location and signal sampling) must exist between individual time steps.
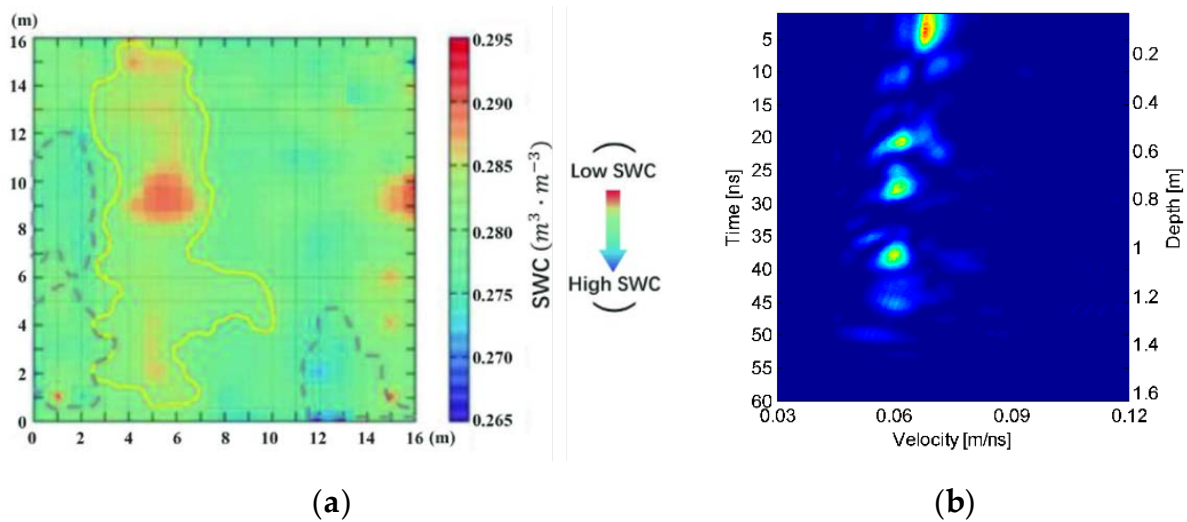
Figure 7. GPR prospecting for SWC estimation. (**a**) SWC distribution determined by the surface reflection method [170]. (**b**) Velocity spectrum resulting from common mid-point acquisition [189].

Concerning the signal processing algorithms, taking advantage of the well-known frequency-dependent behaviour of the GPR signal, the water content estimation has been correlated to a shift in the spectral characteristics of GPR signals [202–206], appreciable through a time–frequency decomposition [207] or through the application of automated learning algorithms [208,209]. Early-time attributes of GPR surface reflection, a method developed to overcome difficulties in separating the overlapping air and ground waves and that is based on the analysis of the envelope of the signal performed in different time windows, has shown some potential in determining the moisture content [210–214]. Since antenna radiation characteristics are affected by the EM properties of the shallower layer, changes in amplitude, shape and time duration of the ground wave signature are expected to occur for changing soil conditions. However, in addition to a limited accuracy for highly heterogeneous soil, it should be mentioned that the early-time signal is affected by both conductivity and dielectric permittivity but that their effects cannot yet be differentiated.

4.3. Soil Textural Properties

In principle, the capability of GPR in providing information on soil texture depends on the magnitude and sharpness of its variation; therefore, it is possible to locate soil horizons with strongly contrasting textures only [215–218]. For this reason, a limited number of works have vertically addressed the topic, resulting in a commonly accepted high-level characterisation of soils into coarse-grained and fine-grained texture [219–221].

To overcome these limitations, considering the small differences in permittivity values described in Table 3, textural estimation has been indirectly obtained from variations in the SWC. In particular, the most successful approach has been the determination of the soil clay content. From a radar perspective, with respect to the other two soil constituents (i.e., silt and sand), clay has a predominant effect on GPR wavelet amplitude and frequency characteristics, as well as producing a relevant increase in soil conductivity [222–224].

Clay content has been successfully delineated at both the field and laboratory scale mainly through two different approaches: the analysis of the early-time GPR signal amplitude (Figure 8a) and the observed signal attenuation; the evaluation of the received signal in the frequency domain. In the latter case, a significant shift towards lower frequencies has been observed for increased clay content [225–230].

Amplitude-based analysis is based on the principle that a signal propagating through a clayey soil is more attenuated, and, therefore, penetration depth decreases. This consideration is at the foundation of the work of Doolittle and Collins [106], where the soil textural properties were indirectly estimated by evaluating the penetration performance of GPR.

Essentially, bearing in mind a quasi-homogeneity assumption, abrupt variations in the recorded amplitude can be associated to soil textural transitions, especially between sand and clay textures [231–237] (Figure 8a).

Effects due to organic matter content are similar to those of clay [238–240]; hence, increased content generally produces a soil with increased water-holding capacity and conductivity [241,242] (Figure 8b). If, on one side, this dependency suggests that measurements of permittivity values could provide a way to estimate the organic content feature [243–247], at the same time it represents a challenge in scenarios where organic matter occurs in association with clay and water [173,248,249]. In those situations, GPR results alone are not able to conclusively resolve the different contributions; therefore, it is not possible to differentiate their impact on the collected GPR signals [250–253]. As a consequence, most of the advancements have been achieved by refining and improving the existing dielectric mixing relationships in order to account for both the soil texture and the organic content [254–256]. Nevertheless, some successful results have been obtained in the case of large impedance contrast through the analysis of GPR wavelet amplitude analysis [257–261].
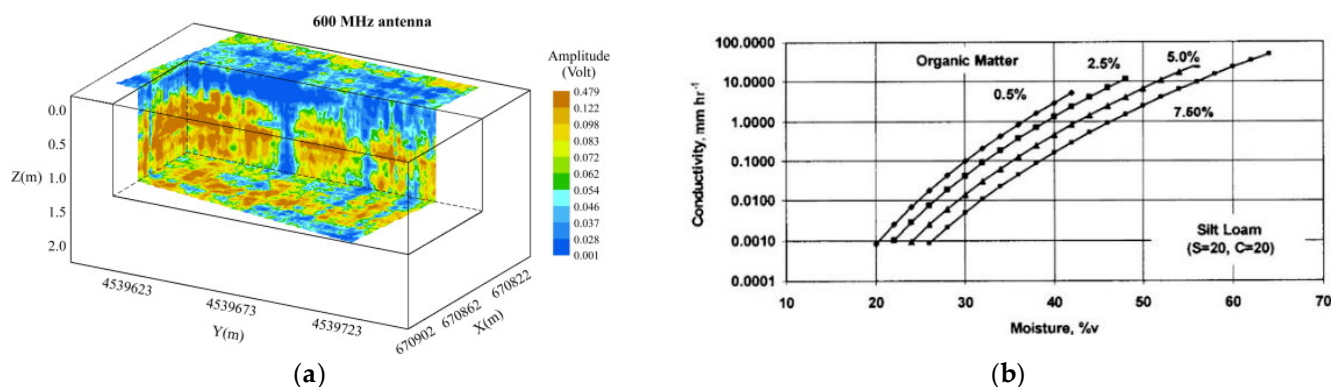

Figure 8. GPR prospecting for soil textural properties. (**a**) Prediction of clay content from analysis of GPR reflection data signal amplitude [236]. (**b**) Variations of soil hydraulic conductivity and moisture by organic matter [251].

4.4. Soil Structural Properties

Identifying soil structural properties, including compaction, porosity, density and vertical stratification in different horizons, represents a task that well matches the operational capabilities of GPR, mainly as a consequence of the fact that the high-resolution feature exhibited by the methodology makes it capable of following the spatial and temporal variations to which such properties are subjected [166,262–264].

Until now, the observation of soil compaction (e.g., decrease in porosity, increase in density and change in soil hydrological properties functions), has been accomplished by exploiting relative changes in soil dielectric constant and EM wave velocity, due to the fact that soil water content varies with soil compaction condition, therefore indirectly affecting dielectric permittivity [265–269] (Figure 9a). The majority of experiments have approached the problem by analysing the wavelet characteristics (amplitude and spectrum) of early-time GPR signals, for which a strong correlation has been found with the dielectric constant, and by establishing the corresponding empirical relationships [270–279].

Due to the direct impact that the structural properties have on the mechanical ones, several works have combined in situ mechanical and penetrometric probes with GPR measurements, with the primary aim of estimating the required effort for land regeneration processes [280–283].
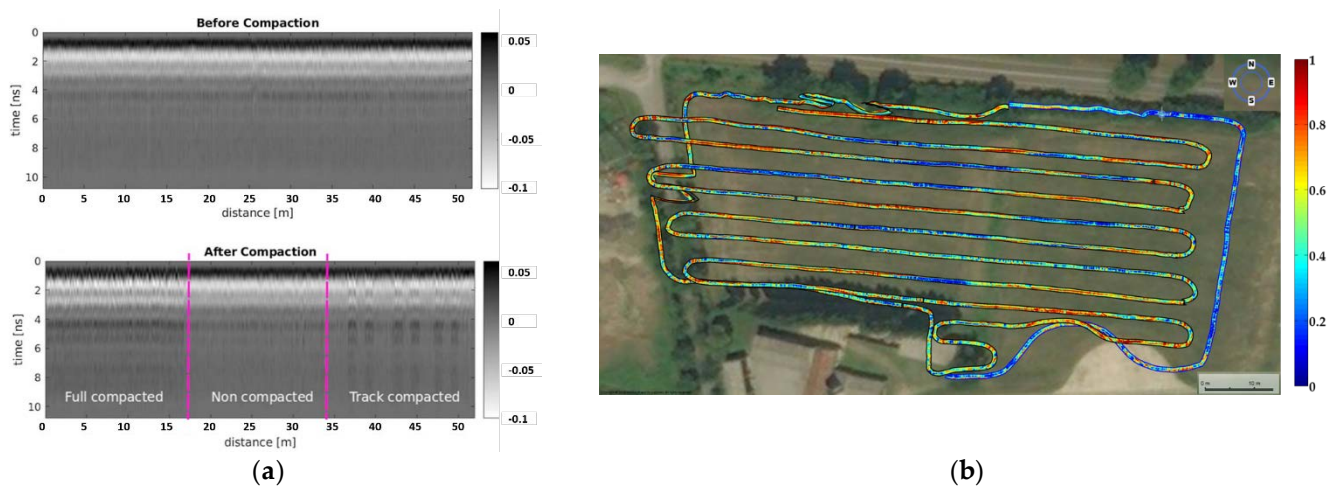
Figure 9. GPR prospecting for soil structural properties. (**a**) Identification of compacted zones in a field experiment [251]. (**b**) Delineation of highly reflective morphological anomalies through the analysis of the GPR amplitude characteristics (red to blue colour scale) [269].

What all these studies have in common is the fact that they demonstrated the suitability of GPR in detecting soil layers affected by compaction, or generally to detect less permeable layers (Figure 9b), but at the same time they highlight the necessity of adequate and additional ground truth data to retrieve an accurate relationship between soil compaction and GPR signal, as well as the knowledge of previous or current land use. For these reasons, conducted research typically involved dedicated compaction-induced processes and sample collections for calibration.

The characterisation of porosity features has been usually obtained through the analysis of GPR reflection amplitude in combination with a number of petrophysical relationships and signal inversion models to convert the measured dielectric permittivity into porosity information [284–288]. In addition, wave velocity variations due to the differences in porosity have been tracked through common mid-point and wide-angle reflection and refraction acquisition schemes [289–293] and cross-hole tomography [294–297]. To improve the accuracy of the process, Full Wave Inversion (FWI) techniques [298–301] and automated feature extraction schemes [302,303] have also been developed.

4.5. Soil Hydraulic Properties

For what concerns the characterisation of the soil hydraulic parameters (Figure 10), mainly represented by the soil water retention and hydraulic conductivity functions [304–308], the majority of works in the literature have been carried out at laboratory or small scales [309], with the main purpose of developing accurate hydrodynamic models that could match pedotransfer functions and experimental data [310–312]. Reference models have been developed in [34,313,314]. In particular, the characterisation of soil hydraulic conductivity has been typically accomplished through the analysis of the observed signal attenuation in both unsaturated and saturated soil samples, as well as by processing time-lapse GPR data, and in particular GPR groundwave data, in search for changes in SWC with time [315–319]. The estimations are then coupled with the analytical relationships previously mentioned (principally the Van Genuchten model and its modifications) to finally obtain a soil-specific empirical description. The determination of the parameters involved in the analytical formulations is usually performed by artificially forcing a saturated soil condition, either through artificial infiltration, percolation or infiltrometer methods [320–324], in which the volume of infiltrated water versus time is fitted to infer soil hydraulic conductivity at or close to saturation. However, in addition to being time-consuming and difficult to replicate on a large scale, such methodologies are limited by a significant uncertainty in accurately contouring the infiltration bulb shape.
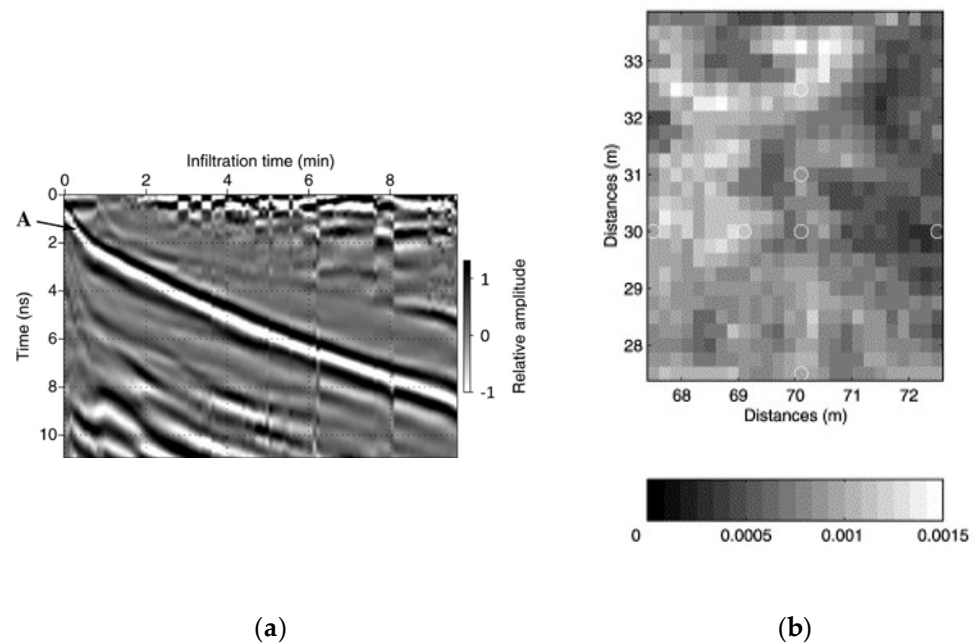
(a) **(b)**

Figure 10. GPR prospecting for soil hydraulic properties. (**a**) Time-lapse GPR data acquired during constant head infiltration (reflection A is the wetting front) [305]. (**b**) Estimated horizontal distribution of hydraulic conductivity in a saturated sand layer using common mid-point velocity estimation and Kozeny–Carman relationships [311].

A similar approach has been followed to identify the parametrisation of the soil water retention curve, i.e., its functional form [325–328]. Specifically, the soil water retention curve relates the soil water pressure head to its volumetric water content, and its shape is determined by soil texture and pore size distribution. Considering that wave propagation velocity decreases due to an increase in water content and the signal frequency spectra allows us to characterise the unsaturated and the transition zone [329,330], GPR data inversion has been applied to find the water retention curve parameters. GPR reflection measurements have been successfully adopted to determine the location of the groundwater table, while numerical models have been developed to estimate the wave propagation in the transition zone. By combining these results and the analytical relationships previously mentioned, it is possible to reconstruct the water retention curve by data fitting [48,331–338]. Despite showing promising results, significant errors have been observed for deeper layers, where noise in the measurements drastically reduces the accuracy of the inversion schemes. In addition, a great deal of ancillary information is required to optimise the conceptual design of the GPR inversion model, such as details on soil texture, compositions and stratigraphy [339,340].

These results indicate that GPR is a useful tool to capture the trend in hydraulic conductivity and retention with reasonable accuracy for agricultural applications at the field scale, but the estimation of the actual values is still subject to high variability due to the assumptions and simplifications that are included in the inversion model, such as homogeneity, isotropy and non-dispersive 1D propagation [326,328].

Finally, very few works have addressed the determination of critical SWC values, such as soil WP and soil water content at Field Capacity (FC), needed to determine the available water capacity. The main reasons for this are the fact these soil hydraulic conditions are temporary and not uniformly distributed in the field given soil heterogeneity (FC), and difficult to reach in real field conditions (WP) [341,342]. Moreover, WP depends not only on the soil hydric regime, but also on the interaction with crop type [343,344].

Works on the topic have mainly addressed the development of specific dielectric mixing models, or the modification of existing ones, that could account for this feature when building the forward model of the permittivity values to soil water content. The

estimation of the available water content property is then performed by matching the model functions with surface soil moisture measurements, obtained either through GPR reflection or early-time signal analysis [345–348]. Given the limitations of GPR in providing an absolute value of water content alone, i.e., without relying on external or ancillary information, it is clear that all the processes that follow will hardly produce quantitative representation of the exploited feature.

5. Discussion

The principal outcome that can be derived from the exploited panorama is the fact that the majority of the described soil parameters stem, directly or indirectly, from the measurement of the soil water content feature, which clearly represents the most-researched attribute. Under the assumptions that variations in the apparent soil permittivity and conductivity are dominated by changes in the water content, such information has been mainly retrieved through the analysis of the variations in GPR wave velocity and reflection coefficient magnitude. Though theoretically reasonable, the mentioned hypothesis means that small-scale spatial heterogeneities, lateral effects, interdependencies and mutual correlation among different parameters (textural or small structural changes and organic contents) are often overlooked, if not completely neglected.

This is exemplified by the achieved results in the field of textural attribute characterisation, where most of the research has been carried out to improve and refine the existing dielectric mixing and pedotransfer relationships. Considering that, up to some degree, sand, silt and clay exhibit a comparable effect on soil permittivity and conductivity, their individual contribution to the GPR wave characteristics can hardly be separated, thus limiting the extraction of information from the GPR profile alone.

This last point is even more stressed for the extraction of specific values or soil conditions, which is typically performed by inverting functions and detailed models to obtain the distribution of subsurface permittivity and conductivity. Between these two situations, research carried out on soil structural property classification, and in particular on soil density and compaction attributes, has shown that it is possible to infer the physical attributes from the interpretation of GPR results, despite being through the detection of relevant changes in the amplitude characteristics of GPR images.

Finally, it can be stated that GPR has proven its validity in providing deeper information on subsurface properties variations than those from alternative geophysical methodologies. On top of that, the possibility of densely surveying large 3D areas in a timely fashion thanks to the deployment of multi-channel systems represents a relevant operational benefit towards its implementation for irrigation optimisation to ensure water sustainability and enhanced agricultural productivity. The ability to obtain dense estimates of soil features holds potential for improving agricultural ecosystem investigation and, hence, the delineation of MZs, at the same time limiting resource wasting. Moreover, the higher the sensitivity of the crop to soil moisture, the larger the benefits will be in employing the GPR methodology.

6. Conclusions

The accurate characterisation of the spatial and temporal variation of soil properties (texture, structure and hydraulic) at the field scale, as well as the determination of soil moisture dynamics, are fundamental in PA. This contribution has reviewed the current state of the GPR research for applications in precision agriculture, and specifically for the domain of water management and precision irrigation. After a preliminary excursus on the motivations that have pushed the deployment of sustainable agricultural techniques and practices, this review has assessed the role that geophysical measurements have played throughout the last decades and beyond.

In particular, the focus has been put on the different operational and processing approaches and methodologies developed to characterise textural, structural and hydraulic

soil properties, which affect the electromagnetic behaviour of soils and can, therefore, be inferable from GPR profiling results.

Summarising the outcomes of the review, it can be concluded that the field of precision farming, despite being extensively developed by the introduction of proximal geophysical sensors, poses a fundamental challenge that still hampers a full exploitation of the potential of the GPR technique, mainly with respect to the data interpretation capability: the natural heterogeneity of soils. Wave propagation, amplitude absorption and GPR reflections are due not only to soil water content, but they are also impacted by other factors that might occur at different temporal and spatial scales, as well as with different magnitude. Therefore, the difficulty in separating and isolating the different contributions is clear, which in turns could cause uncertainties in soil parametrisation and classification. Advanced modelling and wave inversion schemes have clearly mitigated the impact of such errors, but they still suffer from several assumptions, including homogeneity or geometrical simplification, and severe computational requirements. Opportunities exist within the domain of quantitative analysis, with the intent of increasing the level of information that can be extracted from the received signal, as well as from the integration of GPR and other techniques, including semi-invasive ones, as a means to better constrain the problem and reach a more accurate solution. In particular, acknowledging the main limitation that each subsurface layer can respond to more than one soil property variation, combining conceptually different sensing techniques, and, hence, put emphasis on different soil properties, holds the promise of improving the accuracy in property estimates. Such an approach could lead to the investigation of a wide range of physical, chemical and mechanical characteristics, which in turn will allow for a deeper understanding of soil relationships.

Author Contributions: Conceptualization, F.L., A.F., B.O., M.L.; writing—original draft preparation, F.L., A.F., B.O., M.L.; writing—review and editing, F.L., A.F., B.O., M.L. All authors have read and agreed to the published version of the manuscript.

References

1. United Nations Department of Economic and Social Affairs, Population Division. *World Population Prospects 2022: Summary of Results*; UN DESA/POP/2022/TR/NO. 3; United Nations: New York, NY, USA, 2022.
2. FAO. *World Food and Agriculture—Statistical Yearbook 2020*; FAO: Rome, Italy, 2020. [CrossRef]
3. European Commission, Knowledge for Policy. Available online: https://knowledge4policy.ec.europa.eu/foresight/topic/continuing-urbanisation/developments-and-forecasts-on-continuing-urbanisation_en (accessed on 27 November 2022).
4. Xu, D.; Yang, F.; Yu, L.; Zhou, Y.; Li, H.; Ma, J.; Huang, J.; Wei, J.; Xu, Y.; Zhang, C.; et al. Quantization of the coupling mechanism between eco-environmental quality and urbanization from multisource remote sensing data. *J. Clean. Prod.* **2021**, *321*, 128948. [CrossRef]
5. Yin, H.; Cao, Y.; Marelli, B.; Zeng, X.; Mason, A.J.; Cao, C. Soil sensors and plant wearables for smart and precision agriculture. *Adv. Mater.* **2021**, *33*, 2007764. [CrossRef] [PubMed]
6. Singh, U.; Praharaj, C.S.; Gurjar, D.S.; Kumar, R. Precision irrigation management: Concepts and applications for higher use efficiency in field crops. In *Scaling Water Productivity and Resource Conservation in Upland Field Crops Ensuring More Crop per Drop*; ICAR-Indian Institute of Pulses Research: Kampur, India, 2019.
7. Vories, E.; O'Shaughnessy, S.; Sudduth, K.; Evett, S.; Andrade, M.; Drummond, S. Comparison of precision and conventional irrigation management of cotton and impact of soil texture. *Precis. Agric.* **2021**, *22*, 414–431. [CrossRef]
8. Piccoli, I.; Furlan, L.; Lazzaro, B.; Morari, F. Examining conservation agriculture soil profiles: Outcomes from northeastern Italian silty soils combining indirect geophysical and direct assessment methods. *Eur. J. Soil Sci.* **2020**, *71*, 1064–1075. [CrossRef]
9. Moral, F.J.; Serrano, J.M. Using low-cost geophysical survey to map soil properties and delineate management zones on grazed permanent pastures. *Precis. Agric.* **2019**, *20*, 1000–1014. [CrossRef]
10. Frolking, S.; Qiu, J.; Boles, S.; Xiao, X.; Liu, J.; Zhuang, Y.; Li, C.; Qin, X. Combining remote sensing and ground census data to develop new maps of the distribution of rice agriculture in China. *Glob. Biogeochem. Cycles* **2002**, *16*, 38–41. [CrossRef]

11. Youssef, Y.M.; Gemail, K.S.; Sugita, M.; AlBarqawy, M.; Teama, M.A.; Koch, M.; Saada, S.A. Natural and anthropogenic coastal environmental hazards: An integrated remote sensing, GIS, and geophysical-based approach. *Surv. Geophys.* **2021**, *42*, 1109–1141. [CrossRef]

12. Roy, P.C.; Guber, A.; Abouali, M.; Nejadhashemi, A.P.; Deb, K.; Smucker, A.J. Crop yield simulation optimization using precision irrigation and subsurface water retention technology. *Environ. Model. Softw.* **2019**, *119*, 433–444. [CrossRef]

13. De Lara, A.; Khosla, R.; Longchamps, L. Characterizing spatial variability in soil water content for precision irrigation management. *Agronomy* **2018**, *8*, 59. [CrossRef]

14. Neupane, J.; Guo, W. Agronomic basis and strategies for precision water management: A review. *Agronomy* **2019**, *9*, 87. [CrossRef]

15. Batchelor, W.D.; Basso, B.; Paz, J.O. Examples of strategies to analyze spatial and temporal yield variability using crop models. *Eur. J. Agron.* **2002**, *18*, 141–158. [CrossRef]

16. Friedman, S.P. Soil properties influencing apparent electrical conductivity: A review. *Comput. Electron. Agric.* **2005**, *46*, 45–70. [CrossRef]

17. Pradipta, A.; Soupios, P.; Kourgialas, N.; Doula, M.; Dokou, Z.; Makkawi, M.; Alfarhan, M.; Tawabini, B.; Kirmizakis, P.; Yassin, M. Remote Sensing, Geophysics, and Modeling to Support Precision Agriculture—Part 1: Soil Applications. *Water* **2022**, *14*, 1158. [CrossRef]

18. Pradipta, A.; Soupios, P.; Kourgialas, N.; Doula, M.; Dokou, Z.; Makkawi, M.; Alfarhan, M.; Tawabini, B.; Kirmizakis, P.; Yassin, M. Remote Sensing, Geophysics, and Modeling to Support Precision Agriculture—Part 2: Irrigation Management. *Water* **2022**, *14*, 1157. [CrossRef]

19. Capello, M.A.; Shaughnessy, A.; Caslin, E. The geophysical sustainability atlas: Mapping geophysics to the UN Sustainable Development Goals. *Lead. Edge* **2021**, *40*, 10–24. [CrossRef]

20. Becker, S.M.; Franz, T.E.; Abimbola, O.; Steele, D.D.; Flores, J.P.; Jia, X.; Scherer, T.F.; Rudnick, D.R.; Neale, C.M. Feasibility assessment on use of proximal geophysical sensors to support precision management. *Vadose Zone J.* **2022**, *21*, e20228. [CrossRef]

21. Garré, S.; Hyndman, D.; Mary, B.; Werban, U. Geophysics conquering new territories: The rise of "agrogeophysics". *Vadose Zone J.* **2015**, *20*, e20115. [CrossRef]

22. Freeland, R.S.; Wells, L.G.; Dodd, R.B. Assessing soil properties for site-specific agriculture using ground penetrating radar. In Proceedings of the 9th EEGS Symposium on the Application of Geophysics to Engineering and Environmental Problems, Keystone, CO, USA, 28 April–2 May 1996; p. cp-205. [CrossRef]

23. Radcliffe, D.E.; Šimunek, J. *Soil Physics with HYDRUS, Modeling and Applications*; CRC Press: Boca Raton, FL, USA, 2010.

24. Miller, B.A.; Koszinski, S.; Wehrhan, M.; Sommer, M. Comparison of spatial association approaches for landscape mapping of soil organic carbon stocks. *Soil* **2015**, *1*, 217–233. [CrossRef]

25. Soane, B.D.; van Ouwerkerk, C. Soil Compaction Problems in World Agriculture. In *Developments in Agricultural Engineering*; Elsevier: Amsterdam, The Netherlands, 1994; Volume 11, pp. 1–21.

26. Soane, B.D.; Van Ouwerkerkb, C. Implications of Soil Compaction in Crop Production for the Quality of the Environment. *Soil Tillage Res.* **1995**, *35*, 5–22. [CrossRef]

27. Horna, R.; Domialb, H.; Slowihka-Jurkiewiczb, A.; Van Ouwerkerkct, C. Soil Compaction Processes and Their Effects on the Structure of Arable Soils and the Environment. *Soil Tillage Res.* **1995**, *35*, 23–36. [CrossRef]

28. Lipiec, J.; Stcpniewski, W. Effects of Soil Compaction and Tillage Systems on Uptake and Losses of Nutrients. *Soil Tillage Res.* **1995**, *35*, 37–52. [CrossRef]

29. Taylor, H.; Brar, G. Effect of soil compaction on root development. *Soil Tillage Res.* **1991**, *19*, 111–119. [CrossRef]

30. Osman, K.T. *Soils: Principles, Properties and Management*; Springer: New York, NY, USA, 2013.

31. Romero-Ruiz, A.; Linde, N.; Baron, L.; Solazzi, S.G.; Keller, T.; Or, D. Seismic signatures reveal persistence of soil compaction. *Vadose Zone J.* **2021**, *20*, e20140. [CrossRef]

32. Kutílek, M.; Nielsen, D.R. *Soil Hydrology*; Catena Verl: Reiskirchen, Germany, 1994.

33. Brooks, R.H.; Corey, A.T. *Hydraulic Properties of Porous Media*; Hydrology Paper 3; Colorado St. University: Fort Collins, CO, USA, 1964.

34. Van Genuchten, M.T. A closed-form equation for predicting the hydraulic conductivity of unsaturated soils. *Soil Sci. Soc. Am. J.* **1980**, *44*, 892–898. [CrossRef]

35. Tietje, O.; Tapkenhinrichs, M. Evaluation of pedotransfer functions. *Soil Sci. Soc. Am. J.* **1993**, *57*, 1088–1095. [CrossRef]

36. Cornelis, W.M.; Ronsyn, J.; Meirvenne, M.V.; Hartmann, R. Evaluation of pedotranfer functions for predicting the soil moisture retention curve. *Soil Sci. Soc. Am. J.* **2001**, *65*, 638–648. [CrossRef]

37. Pachepsky, Y.; Rawls, W.J. Development of pedotransfer functions in soil hydrology. In *Developments in Soil Science*; Elsevier Science: Amsterdam, The Netherlands, 2004; Volume 30.

38. Soil Science Division Staff. *Soil Survey Manual*; Ditzler, C., Scheffe, K., Monger, H.C., Eds.; USDA Handbook 18; Government Printing Office: Washington, DC, USA, 2017.

39. Rawls, W.J.; Brakensiek, D.L.; Soni, B. Agricultural management effects on soil water processes part I: Soil water retention and Green and Ampt parameters. *Trans. ASAE* **1983**, *26*, 1747–1752. [CrossRef]

40. Rawls, W.J.; Brakensiek, D.L. Estimation of soil water retention and hydraulic properties. In *Unsaturated Flow in Hydrologic Modeling*; Springer: Dordrecht, The Netherlands, 1989; pp. 275–300.

41. Patil, N.G.; Singh, S.K. Pedotransfer functions for estimating soil hydraulic properties: A review. *Pedosphere* **2016**, *26*, 417–430. [CrossRef]

42. Rawls, W.J.; Brakensiek, D.L. Prediction of soil water properties for hydrologic modeling. In Proceedings of the Symposium on Watershed Management in the Eighties, New York, NY, USA, 30 April–1 May 1985; Jones, E.E., Ward, T.J., Eds.; ASCE Convention: Anaheim, CA, USA, 1985; pp. 293–299.

43. Rawls, W.J. Estimating soil bulk density from particle size analysis and organic matter content. *Soil Sci.* **1983**, *135*, 123–125. [CrossRef]

44. Saxton, K.E.; Rawls, W.J.; Romberger, J.S.; Papendick, R.I. Estimating generalized soil-water characteristics from texture. *Soil Sci. Soc. Am. J.* **1986**, *50*, 1031–1035. [CrossRef]

45. Saxton, K.E.; Rawls, W.J. Soil water characteristic estimates by texture and organic matter for hydrologic solutions. *Soil Sci. Soc. Am. J.* **2006**, *70*, 1569–1578. [CrossRef]

46. Wosten, J.H.M.; Lilly, A.; Nemes, A.; Bas, C.L. Development and use of a database of hydraulic properties of European soils. *Geoderma* **1999**, *90*, 169–185. [CrossRef]

47. Schaap, M.G.; Leij, F.J.; van Genuchten, M.T. ROSETTA: A computer program for estimating soil hydraulic parameters with hierarchical pedotransfer functions. *J. Hydrol.* **2001**, *251*, 163–176. [CrossRef]

48. Zhang, Y.; Schaap, M.G. Weighted recalibration of the Rosetta pedotransfer model with improved estimates of hydraulic parameter distributions and summary statistics (Rosetta3). *J. Hydrol.* **2017**, *547*, 39–53. [CrossRef]

49. Rawls, W.J.; Brakensiek, D.L.; Saxton, K.E. Estimation of soil water properties. *Trans. ASAE* **1982**, *25*, 1316–1320+1328. [CrossRef]

50. Corwin, D.L.; Lesch, S.M. Application of soil electrical conductivity to precision agriculture: Theory, principles, and guidelines. *Agron. J.* **2003**, *95*, 455–471. [CrossRef]

51. Klein, K.A.; Santamarina, J.C. Electrical conductivity in soils: Underlying phenomena. *J. Environ. Eng. Geophys.* **2003**, *8*, 263–273. [CrossRef]

52. Rehman, F.; Abouelnaga, H.S.O.; Rehman, F. Estimation of dielectric permittivity, water content, and porosity for environmental engineering and hydrogeological studies using ground penetrating radar, a short review. *Arab. J. Geosci.* **2016**, *9*, 312. [CrossRef]

53. Brovelli, A.; Cassiani, G. Combined estimation of effective electrical conductivity and permittivity for soil monitoring. *Water Resour. Res.* **2011**, *47*, W08510. [CrossRef]

54. Fukue, M.; Minato, T.; Horibe, H.; Taya, N. The micro-structure of clay given by resistivity measurements. *Eng. Geol.* **1999**, *54*, 43–53. [CrossRef]

55. Hendrickx, J.M.H.; Das, B.; Corwin, D.L.; Wraith, J.M.; Kachanoski, R.G. Relationship between soil water solute concentration and apparent soil electrical conductivity. In *Methods of Soils Analysis: Part 4. Physical Methods*; Dane, J.H., Topp, J.C., Eds.; Soil Science Society of America: Madison, WI, USA, 2002; pp. 1275–1282.

56. Samouëlian, A.; Cousin, I.; Tabbagh, A.; Bruand, A.; Richard, G. Electrical resistivity survey in soil science: A review. *Soil Tillage Res.* **2005**, *83*, 173–193. [CrossRef]

57. Kweon, G.; Lund, E.; Maxton, C. Soil organic matter and cation-exchange capacity sensing with on-the-go electrical conductivity and optical sensors. *Geoderma* **2013**, *199*, 80–89. [CrossRef]

58. Besson, A.; Cousin, I.; Samouëlian, A.; Boizard, H.; Richard, G. Structural heterogeneity of the soil tilled layer as characterized by 2D electrical resistivity surveying. *Soil Tillage Res.* **2004**, *79*, 239–249. [CrossRef]

59. Keller, G.V.; Frischknecht, F.C. *Electrical Methods in Geophysical Prospecting*; Pergamon: New York, NY, USA, 1966.

60. Hilhorst, M.A. *Dielectric Characterization of Soil*; Wageningen Agricultural University: Wageningen, The Netherlands, 1998.

61. Topp, G.C.; Davis, J.L.; Annan, A.P. Electromagnetic determination of soil water content: Measurements in coaxial transmission lines. *Water Resour. Res.* **1980**, *16*, 574–582. [CrossRef]

62. Jadoon, K.Z.; Slob, E.; Vanclooster, M.; Vereecken, H.; Lambot, S. Uniqueness and stability analysis of hydrogeophysical inversion for time-lapse ground penetrating radar estimates of shallow soil hydraulic properties. *Water Resour. Res.* **2008**, *44*, W09421. [CrossRef]

63. Kowalsky, M.B.; Finsterle, S.; Peterson, J.; Hubbard, S.; Rubin, Y.; Majer, E.; Ward, A.; Gee, G. Estimation of field-scale soil hydraulic and dielectric parameters through joint inversion of GPR and hydrological data. *Water Resour. Res.* **2005**, *41*, W11425. [CrossRef]

64. Lambot, S.; Slob, E.C.; Vanclooster, M.; Vereecken, H. Closed loop GPR data inversion for soil hydraulic and electric property determination. *Geophys. Res. Lett.* **2006**, *33*, L21405. [CrossRef]

65. Allred, B.; Daniels, J.J.; Ehsani, M.R. (Eds.) *Handbook of Agricultural Geophysics*, 1st ed.; CRC Press: Boca Raton, FL, USA, 2008. [CrossRef]

66. Adamchuk, V.I.; Hummel, J.W.; Morgan, M.T.; Upadhyaya, S.K. On-the-go soil sensors for precision agriculture. *Comput. Electron. Agric.* **2004**, *44*, 71–91. [CrossRef]

67. Archie, G.E. The electrical resistivity log as an aid in determining some reservoir characteristics. *Trans. Am. Inst. Min. Metall. Pet. Eng.* **1942**, *146*, 54–62. [CrossRef]

68. Briggs, L.J. *Electrical Instruments for Determining the Moisture, Temperature, and Soluble Salts Content of Soils*; USDA Division of Soils Bulletin 10; U.S. Government Printing Office: Washington, DC, USA, 1899.

69. Smith-Rose, R.L. The electrical properties of soil for alternating currents at radio frequencies. *Proc. R. Soc. Lond.* **1933**, *140*, 359–377. [CrossRef]

70. Hulin, G.; Maneuvrier, C.; Tabbagh, A.; Vincent, J.B. What exists beneath the place where Conrad Schlumberger carried out the first (1912) electrical prospection experiment: The Val-Richer Abbey. *Near Surf. Geophys.* **2018**, *16*, 445–460. [CrossRef]

71. Schlumberger, C. *Premières Expériences. Carte des Courbes Equi-Potentielles, Tracées au Courant Continu Val-Richer (Calvados)*; Ref 4717; Musée de Crèvecoeur en Auge: Calvados, France, 1912.

72. Wenner, F. *A Method of Measuring Earth Resistivity (No. 258)*; US Government Printing Office: Washington, DC, USA, 1916.

73. Rhoades, J.D.; Ingvalson, R.D. Determining salinity in field soils with soil resistance measurements. *Proc. Soil Sci. Soc. Am. J.* **1971**, *35*, 54–60. [CrossRef]

74. Edlefsen, N.E.; Anderson, A.B.C. The four-electrode resistance method for measuring soil moisture content under field conditions. *Soil Sci.* **1941**, *51*, 367–376. [CrossRef]

75. McNeill, J.D.; Black, G.D.; Bosnar, M. Method and Apparatus for Measuring Terrain Resistivity. U.S. Patent US4070612A, 2 June 1976. Available online: https://patents.google.com/patent/US4070612A/en (accessed on 27 November 2022).

76. Williams, B.G.; Baker, G.C. An electromagnetic induction technique for reconnaissance surveys of soil salinity hazards. *Soil Res.* **1982**, *20*, 107–118. [CrossRef]

77. Rhoades, J.D.; Corwin, D.L. Determining soil electrical conductivity-depth relations using an inductive electromagnetic soil conductivity meter. *Soil Sci. Soc. Am. J.* **1981**, *45*, 255–260. [CrossRef]

78. de Jong, E.; Ballantyne, A.K.; Caneron, D.R.; Read, D.W. Measurement of apparent electrical conductivity of soils by an electromagnetic induction probe to aid salinity surveys. *Soil Sci. Soc. Am. J.* **1979**, *43*, 810–812. [CrossRef]

79. Doolittle, J.A.; Brevik, E.C. The use of electromagnetic induction techniques in soils studies. *Geoderma* **2014**, *223*, 33–45. [CrossRef]

80. Triantafilis, J.; Terhune Iv, C.H.; Santos, F.M. An inversion approach to generate electromagnetic conductivity images from signal data. *Environ. Model. Softw.* **2013**, *43*, 88–95. [CrossRef]

81. Morris, E.R. Height-above-ground effects on penetration depth and response of electromagnetic induction soil conductivity meters. *Comput. Electron. Agric.* **2009**, *68*, 150–156. [CrossRef]

82. Corwin, D.L.; Lesch, S.M.; Shouse, P.J.; Soppe, R.; Ayars, J.E. Identifying soil properties that influence cotton yield using soil sampling directed by apparent soil electrical conductivity. *Agron. J.* **2003**, *95*, 352. [CrossRef]

83. Moral, F.J.; Terrón, J.M.; Marques da Silva, J.R. Delineation of management zones using mobile measurements of soil apparent electrical conductivity andmultivariate geostatistical techniques. *Soil Tillage Res.* **2010**, *106*, 335–343. [CrossRef]

84. Scudiero, E.; Teatini, P.; Corwin, D.L.; Deiana, R.; Berti, A.; Morari, F. Delineation of site-specific management units in a saline region at the Venice Lagoon margin, Italy, using soil reflectance and apparent electrical conductivity. *Comput. Electron. Agric.* **2013**, *99*, 54–64. [CrossRef]

85. André, F.; Van Leeuwen, C.; Saussez, S.; Van Durmen, R.; Bogaert, P.; Moghadas, D.; De Resseguier, L.; Delvaux, B.; Vereecken, H.; Lambot, S. High-resolution imaging of a vineyard in south of France using ground-penetrating radar, electromagnetic induction and electrical resistivity tomography. *J. Appl. Geophys.* **2012**, *78*, 113–122. [CrossRef]

86. Doolittle, J.A.; Indorante, S.J.; Potter, D.K.; Hefner, S.G.; McCauley, W.M. Comparing three geophysical tools for locating sand blows in alluvial soils of southeast Missouri. *J. Soil Water Conserv.* **2002**, *57*, 175–182.

87. Fortes, R.; Millán, S.; Prieto, M.H.; Campillo, C. A methodology based on apparent electrical conductivity and guided soil samples to improve irrigation zoning. *Precis. Agric.* **2015**, *16*, 441–454. [CrossRef]

88. Hedley, C.B.; Bradbury, S.; Ekanayake, J.; Yule, I.J.; Carrick, S. Spatial irrigation scheduling for variable rate irrigation. *Proc. N. Z. Grassl. Assoc.* **2010**, *72*, 97–102. [CrossRef]

89. Hedley, C.B.; Roudier, P.; Yule, I.J.; Ekanayake, J.; Bradbury, S. Soil water status and water table depth modelling using electromagnetic surveys for precision irrigation scheduling. *Geoderma* **2013**, *199*, 22–29. [CrossRef]

90. Priori, S.; Martini, E.; Andrenelli, M.C.; Magini, S.; Agnelli, A.E.; Bucelli, P.; Biagi, M.; Pellegrini, S.; Costantini, E.A.C. Improving wine quality through harvest zoning and combined use of remote and soil proximal sensing. *Soil Sci. Soc. Am. J.* **2013**, *77*, 1338–1348. [CrossRef]

91. Ortuani, B.; Facchi, A.; Mayer, A.; Bianchi, D.; Bianchi, A.; Brancadoro, L. Assessing the effectiveness of variable-rate drip irrigation on water use efficiency in a Vineyard in Northern Italy. *Water* **2019**, *11*, 1964. [CrossRef]

92. Ortuani, B.; Facchi, A.; Mayer, A.; Bianchi, A.; Bianchi, D.; Brancadoro, L. Enhancing water use efficiency in irrigated agriculture through variable rate drip irrigation: The case of a pear orchard in Northern Italy. *Acta Hortic.* **2022**, *1335*, 515–522. [CrossRef]

93. Allred, B.J.; Freeland, R.S.; Farahani, H.J.; Collins, M.E. Agricultural geophysics: Past, present, and future. In Proceedings of the 23rd EEGS Symposium on the Application of Geophysics to Engineering and Environmental Problems, Denver, CO, USA, 11–15 April 2010; p. cp-175. [CrossRef]

94. Menshov, O.; Kuderavets, R.; Vyzhva, S.; Chobotok, I.; Pastushenko, T. Magnetic mapping and soil magnetometry of hydrocarbon prospective areas in western Ukraine. *Stud. Geophys. Geod.* **2015**, *59*, 614–627. [CrossRef]

95. Lu, Z.; CHickey, J.; Sabatier, J.M. Effects of compaction on the acoustic velocity in soil. *Soil Sci. Soc. Am. J.* **2004**, *68*, 7–16. [CrossRef]

96. Huang, S.; Lu, C.; Li, H.; He, J.; Wang, Q.; Gao, Z.; Yuan, P.; Li, Y. The attenuation mechanism and regular of the acoustic wave on propagation path in farmland soil. *Comput. Electron. Agric.* **2022**, *199*, 107138. [CrossRef]

97. Xu, Y.; Li, J.; Duan, J.; Song, S.; Jiang, R.; Yang, Z. Soil water content detection based on acoustic method and improved Brutsaert's model. *Geoderma* **2020**, *359*, 114003. [CrossRef]

98. Golovko, L.; Pozdnyakov, A.I. Applications of Self-potential Method in Agriculture. In Proceedings of the 23rd EEGS Symposium on the Application of Geophysics to Engineering and Environmental Problems, Keystone, CO, USA, 11–15 April 2010; p. cp-175. [CrossRef]

99. Jougnot, D.; Linde, N.; Haarder, E.B.; Looms, M.C. Monitoring of saline tracer movement with vertically distributed self-potential measurements at the HOBE agricultural test site, Voulund, Denmark. *J. Hydrol.* **2015**, *521*, 314–327. [CrossRef]

100. Collins, M.E.; Doolittle, J.A. Using ground-penetrating radar to study soil microvariability. *Soil Sci. Soc. Am. J.* **1987**, *51*, 491–493. [CrossRef]

101. Doolittle, J.A.; Asmussen, L.E. Ten years of applications of Ground Penetrating Radar by United States Department of Agriculture. In Proceedings of the Fourth International Conference on Ground Penetrating Radar, Rovaniemi, Finland, 8–13 June 1992; pp. 139–147. [CrossRef]

102. Collins, M.E. *History of Ground-Penetrating Radar Applications in Agriculture*; CRC Press, Taylor and Francis Group: New York, NY, USA, 2008; pp. 45–55.

103. Johnson, R.W.; Glasscum, R.; Wojtasinski, R. Application of ground penetrating radar to soil survey. *Soil Surv. Horiz.* **1982**, *23*, 17–25. [CrossRef]

104. Benson, R.; Glaccum, R. *The Application of Ground-Penetrating Radar to Soil Surveying*; Final Report NASA; Cape Kennedy Space Center: Merritt Island, FL, USA, 1979.

105. Collins, M.E. Soil taxonomy: A useful guide for the application of ground penetrating radar. In Proceedings of the Fourth International Conference on Ground Penetrating Radar, Rovaniemi, Finland, 8–13 June 1992; p. cp-303. [CrossRef]

106. Doolittle, J.A.; Collins, M.E. Use of soil information to determine application of ground penetrating radar. *J. Appl. Geophys.* **1995**, *33*, 101–108. [CrossRef]

107. Doolittle, J.; Dobos, R.; Peaslee, S.; Waltman, S.; Benham, E.; Tuttle, W. Revised ground-penetrating radar soil suitability maps. *J. Environ. Eng. Geophys.* **2010**, *15*, 111–118. [CrossRef]

108. Doolittle, J.A. Using ground-penetrating radar to increase the quality and efficiency of soil surveys. *Soil Surv. Tech.* **1987**, *20*, 11–32. [CrossRef]

109. Shih, S.F.; Doolittle, J.A. Using radar to investigate organic soil thickness in the Florida Everglades. *Soil Sci. Soc. Am. J.* **1984**, *48*, 651–656. [CrossRef]

110. Collins, M.E.; Schellentrager, G.W.; Doolittle, J.A.; Shih, S.F. Using ground-penetrating radar to study changes in soil map unit composition in selected Histosols. *Soil Sci. Soc. Am. J.* **1986**, *50*, 408–412. [CrossRef]

111. Hubbard, R.K.; Asmussen, L.E.; Perkins, H.F. Use of ground-penetrating radar on upland Coastal Plain soils. *J. Soil Water Conserv.* **1990**, *45*, 399–405.

112. Raper, R.L.; Asmussen, L.E.; Powell, J.B. Sensing hard pan depth with ground-penetrating radar. *Trans. ASAE* **1990**, *33*, 0041–0046. [CrossRef]

113. Truman, C.C.; Perkins, H.F.; Asmussen, L.E.; Allison, H.D. Using ground-penetrating radar to investigate variability in selected soil properties. *J. Soil Water Conserv.* **1988**, *43*, 341–345.

114. Smith, M.C.; Vellidis, G.; Thomas, D.L.; Breve, M.A. Measurement of water table fluctuations in a sandy soil using ground penetrating radar. *Trans. ASAE* **1992**, *35*, 1161–1166. [CrossRef]

115. Vellidis, G.; Smith, M.C.; Thomas, D.L.; Asmussen, L.E. Detecting wetting front movement in a sandy soil with ground-penetrating radar. *Trans. ASAE* **1990**, *33*, 1867–1874. [CrossRef]

116. Vellidis, G.; Ghate, S.R.; Asmussen, L.E.; Allison, H.D. *Using Ground-Penetrating Radar (GPR) to Detect Soil Water Movement under Microirrigation Laterals*; No. 90-2534; American Society of Agricultural Engineers: St. Joseph, MI, USA, 1990.

117. Kung, K.J.; Donohue, S.V. Improved solute-sampling protocol in a sandy vadose zone using ground-penetrating radar. *Soil Sci. Soc. Am. J.* **1991**, *55*, 1543–1545. [CrossRef]

118. Lombardi, F.; Podd, F.; Solla, M. From Its Core to the Niche: Insights from GPR Applications. *Remote Sens.* **2022**, *14*, 3033. [CrossRef]

119. Gizzi, F.T.; Leucci, G. Global Research Patterns on Ground Penetrating Radar (GPR). *Surv. Geophys.* **2018**, *39*, 1039–1068. [CrossRef]

120. Knight, R. Ground penetrating radar for environmental applications. *Ann. Rev. Earth Planet. Sci.* **2001**, *29*, 229–255. [CrossRef]

121. Hubbard, S.; Chen, J.; Williams, K.; Rubin, Y.; Peterson, J. Environmental and agricultural applications of GPR. In Proceedings of the 3rd Int Work on Advanced Ground Penetrating Radar, IWAGPR 2005, Delft, The Netherlands, 2–3 May 2005; pp. 45–49. [CrossRef]

122. Zajícová, K.; Chuman, T. Application of ground penetrating radar methods in soil studies: A review. *Geoderma* **2019**, *343*, 116–129. [CrossRef]

123. Liu, X.; Dong, X.; Leskovar, D.I. Ground penetrating radar for underground sensing in agriculture: A review. *Int. Agrophys.* **2016**, *30*, 533–543. [CrossRef]

124. Friedman, S.P. Electrical Properties of Soils. In *Encyclopedia of Agrophysics. Encyclopedia of Earth Sciences Series*; Gliński, J., Horabik, J., Lipiec, J., Eds.; Springer: Dordrecht, The Netherlands, 2011. [CrossRef]

125. Doolittle, J. Ground-Penetrating Radar, Soil Exploration. In *Encyclopedia of Agrophysics. Encyclopedia of Earth Sciences Series*; Gliński, J., Horabik, J., Lipiec, J., Eds.; Springer: Dordrecht, The Netherlands, 2011. [CrossRef]

126. Hoekstra, P.; Delaney, A. Dielectric properties of soils at UHF and microwave frequencies. *J. Geophys. Res.* **1974**, *79*, 1699–1708. [CrossRef]

127. Curtis, J.O. Moisture effects on the dielectric properties of soils. *IEEE Trans. Geosci. Remote Sens.* **2001**, *39*, 125–128. [CrossRef]
128. Szypłowska, A.; Saito, H.; Yagihara, S.; Furuhata, K.; Szerement, J.; Kafarski, M.; Lewandowski, A.; Wilczek, A.; Skierucha, W. Relations between Dielectric Permittivity and Volumetric Water Content of Living Soil. In Proceedings of the 2021 13th International Conference on Electromagnetic Wave Interaction with Water and Moist Substances (ISEMA), Lublin, Poland, 26–30 July 2021; pp. 1–4. [CrossRef]
129. Curtis, J.O.; Weiss, C.A.; Everett, J.B. *Effect of Soil Composition on Complex Dielectric Properties*; Technical Report EL-95-34; U.S. Army Corps of Engineers Waterways Experiment Station: Vicksburg, MS, USA, 1995.
130. Turner, G. GPR and the Effects of Conductivity. *Explor. Geophys.* **1992**, *23*, 381–385. [CrossRef]
131. Malicki, M.A.; Walczak, R.T. Evaluating soil salinity status from bulk electrical conductivity and permittivity. *Eur. J. Soil Sci.* **1999**, *50*, 505–514. [CrossRef]
132. Liu, J.; Liu, Q. Soil Moisture Estimate Uncertainties from the Effect of Soil Texture on Dielectric Semiempirical Models. *Remote Sens.* **2020**, *12*, 2343. [CrossRef]
133. Hipp, J.E. Soil electromagnetic parameters as functions of frequency, soil density, and soil moisture. *Proc. IEEE* **1974**, *62*, 98–103. [CrossRef]
134. Wobschall, D. A theory of the complex dielectric permittivity of soil containing water: The semidisperse model. *IEEE Trans. Geosci. Electron.* **1977**, *15*, 49–58. [CrossRef]
135. Comite, D.; Galli, A.; Lauro, S.E.; Mattei, E.; Pettinelli, E. Analysis of GPR early-time signal features for the evaluation of soil permittivity through numerical and experimental surveys. *IEEE J. Sel. Top. Appl. Earth Obs. Remote Sens.* **2015**, *9*, 178–187. [CrossRef]
136. Liu, X.; Dong, X.; Xue, Q.; Leskovar, D.I.; Jifon, J.; Butnor, J.R.; Marek, T. Ground penetrating radar (GPR) detects fine roots of agricultural crops in the field. *Plant Soil* **2018**, *423*, 517–531. [CrossRef]
137. Steelman, C.M.; Endres, A.L. Assessing vertical soil moisture dynamics using multi-frequency GPR common-midpoint soundings. *J. Hydrol.* **2012**, *436*, 51–66. [CrossRef]
138. Loewer, M.; Igel, J.; Wagner, N. Spectral decomposition of soil electrical and dielectric losses and prediction of in situ GPR performance. *IEEE J. Sel. Top. Appl. Earth Obs. Remote Sens.* **2015**, *9*, 212–220. [CrossRef]
139. Rhebergen, J.B.; Lensen, H.A.; van Wijk, R.; Hendrickx, J.M.; van Dam, R.L.; Borchers, B. Prediction of soil effects on GPR signatures. In Proceedings of the Detection and Remediation Technologies for Mines and Minelike Targets IX, Orlando, FL, USA, 21 September 2004; Volume 5415, pp. 705–715. [CrossRef]
140. Daniels, D.J. Ground Penetrating Radar. In *Encyclopedia of RF and Microwave Engineering*; Chang, K., Ed.; John Wiley & Sons, Inc.: New York, NY, USA, 2005. [CrossRef]
141. Wensink, W.A. Dielectric properties of wet soils in the frequency range 1–3000 MHz1. *Geophys. Prospect.* **1993**, *41*, 671–696. [CrossRef]
142. Alsharahi, G.; Driouach, A.; Faize, A. Performance of GPR influenced by electrical conductivity and dielectric constant. *Procedia Technol.* **2016**, *22*, 570–575. [CrossRef]
143. Freeland, R.S.; Yoder, R.E.; Ammons, J.T. Mapping shallow underground features that influence site-specific agricultural production. *J. Appl. Geophys.* **1998**, *40*, 19–27. [CrossRef]
144. Salat, C.; Junge, A. Dielectric permittivity of fine-grained fractions of soil samples from eastern Spain at 200 MHz. *Geophysics* **2010**, *75*, J1–J9. [CrossRef]
145. Hamdan, H.; Economou, N.; Vafidis, A.; Bano, M.; Ortega-Ramirez, J. A New Approach for Adaptive GPR Diffraction Focusing. *Remote Sens.* **2022**, *14*, 2547. [CrossRef]
146. Noborio, K. Measurement of soil water content and electrical conductivity by time domain reflectometry: A review. *Comput. Electron. Agric.* **2001**, *31*, 213–237. [CrossRef]
147. Liu, J.; Zhao, S.; Jiang, L.; Chai, L.; Wu, F. The influence of organic matter on soil dielectric constant at microwave frequencies (0.5–40 GHZ). In Proceedings of the 2013 IEEE International Geoscience and Remote Sensing Symposium-IGARSS, Melbourne, Australia, 21–26 July 2013; pp. 13–16. [CrossRef]
148. Bradford, J.H. Frequency-dependent attenuation analysis of ground-penetrating radar data. *Geophysics* **2007**, *72*, J7–J16. [CrossRef]
149. Wu, B.; Li, X.; Zhao, K.; Jiang, T.; Zheng, X.; Li, X.; Gu, L.; Wang, X. A nondestructive conductivity estimating method for saline-alkali land based on ground penetrating radar. *IEEE Trans. Geosci. Remote Sens.* **2019**, *58*, 2605–2614. [CrossRef]
150. Wunderlich, T.; Rabbel, W. Attenuation of GPR waves in soil samples based on reflection measurements. In Proceedings of the 2011 6th International Workshop on Advanced Ground Penetrating Radar (IWAGPR), Aachen, Germany, 22–24 June 2011; pp. 1–4. [CrossRef]
151. Nazli, H.; Bicak, E.; Sezgin, M. Experimental investigation of different soil types for buried object imaging using impulse GPR. In Proceedings of the XIII Internarional Conference on Ground Penetrating Radar, Lecce, Italy, 21–25 June 2010; pp. 1–5. [CrossRef]
152. Bano, M. Constant dielectric losses of ground-penetrating radar waves. *Geophys. J. Int.* **1996**, *124*, 279–288. [CrossRef]
153. Noon, D.A.; Stickley, G.F.; Longstaff, D. A frequency-independent characterisation of GPR penetration and resolution performance. *J. Appl. Geophys.* **1998**, *40*, 127–137. [CrossRef]
154. Wunderlich, T.; Rabbel, W. Absorption and frequency shift of GPR signals in sandy and silty soils: Empirical relations between quality factor Q, complex permittivity and clay and water contents. *Near Surf. Geophys.* **2013**, *11*, 117–128. [CrossRef]

155. Lai, W.W. Spectral shift and absorption of GPR signals in a wetted sand column. In Proceedings of the 15th International Conference on Ground Penetrating Radar, Brussels, Belgium, 30 June–4 July 2014; pp. 687–691. [CrossRef]

156. Lauro, S.E.; Baniamerian, J.; Cosciotti, B.; Mattei, E.; Pettinelli, E. Loss tangent estimation from ground-penetrating radar data using Ricker wavelet centroid-frequency shift analysis. *Geophysics* **2022**, *87*, H1–H12. [CrossRef]

157. Nobes, D.C.; Deng, J. Ground Penetrating Radar Resolution in Archaeological Geophysics. In *Archaeogeophysics. Natural Science in Archaeology*; El-Qady, G., Metwaly, M., Eds.; Springer: Cham, Switzerland, 2019. [CrossRef]

158. Belina, F.A.; Dafflon, B.; Tronicke, J.; Holliger, K. Enhancing the vertical resolution of surface georadar data. *J. Appl. Geophys.* **2009**, *68*, 26–35. [CrossRef]

159. Słowik, M. Influence of measurement conditions on depth range and resolution of GPR images: The example of lowland valley alluvial fill (the Obra River, Poland). *J. Appl. Geophys.* **2012**, *85*, 1–14. [CrossRef]

160. Luo, T.X.; Lai, W.W.; Chang, R.K.; Goodman, D. GPR imaging criteria. *J. Appl. Geophys.* **2019**, *165*, 37–48. [CrossRef]

161. Plumb, R.G.; Noon, D.A.; Longstaff, I.D.; Stickley, G.F. A waveform-range performance diagram for ground-penetrating radar. *J. Appl. Geophys.* **1998**, *40*, 117–126. [CrossRef]

162. Liu, L.; Zhu, L. GPR signal analysis: Can we get deep-penetration and high-resolution simultaneously? In Proceedings of the Tenth International Conference on Grounds Penetrating Radar, GPR 2004, Delft, The Netherlands, 21–24 June 2004; Volume 1, pp. 263–265.

163. Hong, W.T.; Kang, S.; Lee, S.J.; Lee, J.S. Analyses of GPR signals for characterization of ground conditions in urban areas. *J. Appl. Geophys.* **2018**, *152*, 65–76. [CrossRef]

164. Dossi, M.; Forte, E.; Pipan, M. Quantitative analysis of GPR signals: Transmitted wavelet, amplitude decay, and sampling-related amplitude distortions. *Pure Appl. Geophys.* **2018**, *175*, 1103–1122. [CrossRef]

165. Bitella, G.; Rossi, R.; Loperte, A.; Satriani, A.; Lapenna, V.; Perniola, M.; Amato, M. Geophysical techniques for plant, soil, and root research related to sustainability. In *The Sustainability of Agro-Food and Natural Resource Systems in the Mediterranean Basin*; Springer: Cham, Switzerland, 2015; pp. 353–372. [CrossRef]

166. Romero-Ruiz, A.; Linde, N.; Keller, T.; Or, D. A review of geophysical methods for soil structure characterization. *Rev. Geophys.* **2018**, *56*, 672–697. [CrossRef]

167. Klotzsche, A.; Jonard, F.; Looms, M.C.; van der Kruk, J.; Huisman, J.A. Measuring soil water content with ground penetrating radar: A decade of progress. *Vadose Zone J.* **2018**, *17*, 1–9. [CrossRef]

168. Hardie, M. Review of Novel and Emerging Proximal Soil Moisture Sensors for Use in Agriculture. *Sensors* **2020**, *20*, 6934. [CrossRef]

169. Dobriyal, P.; Qureshi, A.; Badola, R.; Hussain, S.A. A review of the methods available for estimating soil moisture and its implications for water resource management. *J. Hydrol.* **2012**, *458*, 110–117. [CrossRef]

170. Liu, X.; Chen, J.; Cui, X.; Liu, Q.; Cao, X.; Chen, X. Measurement of soil water content using ground-penetrating radar: A review of current methods. *Int. J. Digit. Earth* **2019**, *12*, 95–118. [CrossRef]

171. Klewe, T.; Strangfeld, C.; Kruschwitz, S. Review of moisture measurements in civil engineering with ground penetrating radar–Applied methods and signal features. *Constr. Build. Mater.* **2021**, *278*, 122250. [CrossRef]

172. Jonard, F.; Mahmoudzadeh, M.; Roisin, C.; Weihermüller, L.; André, F.; Minet, J.; Vereecken, H.; Lambot, S. Characterization of tillage effects on the spatial variation of soil properties using ground-penetrating radar and electromagnetic induction. *Geoderma* **2013**, *207*, 310–322. [CrossRef]

173. André, F.; Jonard, M.; Lambot, S. Non-invasive forest litter characterization using full-wave inversion of microwave radar data. *IEEE Trans. Geosci. Remote Sens.* **2014**, *53*, 828–840. [CrossRef]

174. Zhou, L.; Yu, D.; Wang, Z.; Wang, X. Soil water content estimation using high-frequency ground penetrating radar. *Water* **2019**, *11*, 1036. [CrossRef]

175. Wijewardana, Y.G.N.S.; Galagedara, L.W. Estimation of spatio-temporal variability of soil water content in agricultural fields with ground penetrating radar. *J. Hydrol.* **2010**, *391*, 24–33. [CrossRef]

176. Shamir, O.; Goldshleger, N.; Basson, U.; Reshef, M. Mapping spatial moisture content of unsaturated agricultural soils with ground-penetrating radar. *Int. Arch. Photogramm. Remote Sens. Spat. Inf. Sci.* **2016**, *41*, 1279–1285. [CrossRef]

177. Ercoli, M.; Di Matteo, L.; Pauselli, C.; Mancinelli, P.; Frapiccini, S.; Talegalli, L.; Cannata, A. Integrated GPR and laboratory water content measures of sandy soils: From laboratory to field scale. *Constr. Build. Mater.* **2018**, *159*, 734–744. [CrossRef]

178. Galagedara, L.W.; Parkin, G.W.; Redman, J.D.; Von Bertoldi, P.; Endres, A.L. Field studies of the GPR ground wave method for estimating soil water content during irrigation and drainage. *J. Hydrol.* **2005**, *301*, 182–197. [CrossRef]

179. Hubbard, S.; Grote, K.; Rubin, Y. Mapping the volumetric soil water content of a California vineyard using high-frequency GPR ground wave data. *Lead. Edge* **2002**, *21*, 552–559. [CrossRef]

180. Lunt, I.A.; Hubbard, S.S.; Rubin, Y. Soil moisture content estimation using ground-penetrating radar reflection data. *J. Hydrol.* **2005**, *307*, 254–269. [CrossRef]

181. Serbin, G.; Or, D. Ground-penetrating radar measurement of soil water content dynamics using a suspended horn antenna. *IEEE Trans. Geosci. Remote Sens.* **2004**, *42*, 1695–1705. [CrossRef]

182. Glover, P.W. Archie's law—A reappraisal. *Solid Earth* **2016**, *7*, 1157–1169. [CrossRef]

183. Steelman, C.M.; Endres, A.L. Comparison of petrophysical relationships for soil moisture estimation using GPR ground waves. *Vadose Zone J.* **2011**, *10*, 270–285. [CrossRef]

184. Cao, Q.; Song, X.; Wu, H.; Gao, L.; Liu, F.; Yang, S.; Zhang, G. Mapping the response of volumetric soil water content to an intense rainfall event at the field scale using GPR. *J. Hydrol.* **2020**, *583*, 124605. [CrossRef]

185. Greaves, R.J.; Lesmes, D.P.; Lee, J.M.; Toksöz, M.N. Velocity variations and water content estimated from multi-offset, ground-penetrating radar. *Geophysics* **1996**, *61*, 683–695. [CrossRef]

186. Grote, K.; Hubbard, S.; Rubin, Y. Field-scale estimation of volumetric water content using ground-penetrating radar ground wave techniques. *Water Resour. Res.* **2003**, *39*, 1321. [CrossRef]

187. Hamann, G.; Tronicke, J. Global inversion of GPR traveltimes to assess uncertainties in CMP velocity models. *Near Surf. Geophys.* **2014**, *12*, 505–514. [CrossRef]

188. Saito, H.; Kuroda, S.; Iwasaki, T.; Sala, J.; Fujimaki, H. Estimating infiltration front depth using time-lapse multioffset gathers obtained from ground-penetrating-radar antenna array. *Geophysics* **2021**, *86*, WB51–WB59. [CrossRef]

189. Koyama, C.N.; Liu, H.; Takahashi, K.; Shimada, M.; Watanabe, M.; Khuut, T.; Sato, M. In-situ measurement of soil permittivity at various depths for the calibration and validation of low-frequency SAR soil moisture models by using GPR. *Remote Sens.* **2017**, *9*, 580. [CrossRef]

190. Liu, Y.; Irving, J.; Holliger, K. High-resolution velocity estimation from surface-based common-offset GPR reflection data. *Geophys. J. Int.* **2022**, *230*, 131–144. [CrossRef]

191. Forte, E.; Pipan, M. Review of multi-offset GPR applications: Data acquisition, processing and analysis. *Signal Process.* **2017**, *132*, 210–220. [CrossRef]

192. Alumbaugh, D.; Chang, P.Y.; Paprocki, L.; Brainard, J.R.; Glass, R.J.; Rautman, C.A. Estimating moisture contents in the vadose zone using cross-borehole ground penetrating radar: A study of accuracy and repeatability. *Water Resour. Res.* **2002**, *38*, 45-1–45-12. [CrossRef]

193. Klotzsche, A.; Lärm, L.; Vanderborght, J.; Cai, G.; Morandage, S.; Zörner, M.; Vereecken, H.; van der Kruk, J. Monitoring soil water content using time-lapse horizontal borehole GPR data at the field-plot scale. *Vadose Zone J.* **2019**, *18*, 190044. [CrossRef]

194. Klotzsche, A.; Vereecken, H.; van der Kruk, J. Review of crosshole ground-penetrating radar full-waveform inversion of experimental data: Recent developments, challenges, and pitfalls. *Geophysics* **2019**, *84*, H13–H28. [CrossRef]

195. Yu, Y.; Klotzsche, A.; Weihermüller, L.; Huisman, J.A.; Vanderborght, J.; Vereecken, H.; van der Kruk, J. Measuring vertical soil water content profiles by combining horizontal borehole and dispersive surface ground penetrating radar data. *Near Surf. Geophys.* **2020**, *18*, 275–294. [CrossRef]

196. Yu, Y.; Weihermüller, L.; Klotzsche, A.; Lärm, L.; Vereecken, H.; Huisman, J.A. Sequential and coupled inversion of horizontal borehole ground penetrating radar data to estimate soil hydraulic properties at the field scale. *J. Hydrol.* **2021**, *596*, 126010. [CrossRef]

197. Strobach, E.; Harris, B.D.; Dupuis, J.C.; Kepic, A.W. Time-lapse borehole radar for monitoring rainfall infiltration through podosol horizons in a sandy vadose zone. *Water Resour. Res.* **2014**, *50*, 2140–2163. [CrossRef]

198. Jaumann, S.; Roth, K. Soil hydraulic material properties and layered architecture from time-lapse GPR. *Hydrol. Earth Syst. Sci.* **2018**, *22*, 2551–2573. [CrossRef]

199. Lambot, S.; Slob, E.; Rhebergen, J.; Lopera, O.; Jadoon, K.Z.; Vereecken, H. Remote Estimation of the Hydraulic Properties of a Sand Using Full-Waveform Integrated Hydrogeophysical Inversion of Time-Lapse, Off-Ground GPR Data. *Vadose Zone J.* **2009**, *8*, 743–754. [CrossRef]

200. Scholer, M.; Irving, J.; Looms, M.C.; Nielsen, L.; Holliger, K. Examining the Information Content of Time-lapse Crosshole GPR Data Collected Under Different Infiltration Conditions to Estimate Unsaturated Soil Hydraulic Properties. *Adv. Water Resour.* **2013**, *54*, 38–56. [CrossRef]

201. Busch, S.; Weihermüller, L.; Huisman, J.A.; Steelman, C.M.; Endres, A.L.; Vereecken, H.; Van Der Kruk, J. Coupled hydrogeophysical inversion of time-lapse surface GPR data to estimate hydraulic properties of a layered subsurface. *Water Resour. Res.* **2013**, *49*, 8480–8494. [CrossRef]

202. Anbazhagan, P.; Bittelli, M.; Pallepati, R.R.; Mahajan, P. Comparison of soil water content estimation equations using ground penetrating radar. *J. Hydrol.* **2020**, *588*, 125039. [CrossRef]

203. Benedetto, A.; Benedetto, F. Remote sensing of soil moisture content by GPR signal processing in the frequency domain. *IEEE Sens. J.* **2011**, *11*, 2432–2441. [CrossRef]

204. Benedetto, A. Water content evaluation in unsaturated soil using GPR signal analysis in the frequency domain. *J. Appl. Geophys.* **2010**, *71*, 26–35. [CrossRef]

205. Lambot, S.; Slob, E.C.; Van Den Bosch, I.; Stockbroeckx, B.; Scheers, B.; Vanclooster, M. Estimating soil electric properties from monostatic ground-penetrating radar signal inversion in the frequency domain. *Water Resour. Res.* **2004**, *40*, W04205. [CrossRef]

206. Tran, A.P.; Bogaert, P.; Wiaux, F.; Vanclooster, M.; Lambot, S. High-resolution space–time quantification of soil moisture along a hillslope using joint analysis of ground penetrating radar and frequency domain reflectometry data. *J. Hydrol.* **2015**, *523*, 252–261. [CrossRef]

207. Lai, W.L.; Poon, C.S. GPR data analysis in time-frequency domain. In Proceedings of the 2012 14th International Conference on Ground Penetrating Radar (GPR), Shanghai, China, 4–8 June 2012; pp. 362–366. [CrossRef]

208. Barkataki, N.; Mazumdar, S.; Tiru, B.; Sarma, U. Estimation of soil moisture from GPR data using artificial neural networks. In Proceedings of the 2021 IEEE International Conference on Technology, Research, and Innovation for Betterment of Society (TRIBES), Hong Kong, China, 17–19 December 2021; pp. 1–5. [CrossRef]

209. D'Amico, F.; Guattari, C.; Benedetto, A. GPR signal processing in frequency domain using artificial neural network for water content prediction in unsaturated subgrade. In Proceedings of the XIII Internarional Conference on Ground Penetrating Radar, Lecce, Italy, 21–25 June 2010; pp. 1–6. [CrossRef]

210. Algeo, J.; Van Dam, R.L.; Slater, L. Early-time GPR: A method to monitor spatial variations in soil water content during irrigation in clay soils. *Vadose Zone J.* **2016**, *15*, 1–9. [CrossRef]

211. Pettinelli, E.; Vannaroni, G.; Di Pasquo, B.; Mattei, E.; Di Matteo, A.; De Santis, A.; Annan, A.P. Correlation between near-surface electromagnetic soil parameters and early-time GPR signals: An experimental study. *Geophysics* **2007**, *72*, A25–A28. [CrossRef]

212. Pettinelli, E.; Di Matteo, A.; Beaubien, S.E.; Mattei, E.; Lauro, S.E.; Galli, A.; Vannaroni, G. A controlled experiment to investigate the correlation between early-time signal attributes of ground-coupled radar and soil dielectric properties. *J. Appl. Geophys.* **2014**, *101*, 68–76. [CrossRef]

213. Di Matteo, A.; Elena, P.; Evert, S. Early-time GPR signal attributes to estimate soil dielectric permittivity: A theoretical study. *IEEE Trans. Geosci. Remote Sens.* **2013**, *51*, 1643–1654. [CrossRef]

214. Ferrara, C.; Barone, P.M.; Steelman, C.M.; Pettinelli, E.; Endres, A.I. Monitoring shallow soil water content under natural field conditions using the early-time GPR signal technique. *Vadose Zone J.* **2013**, *12*, 1–9. [CrossRef]

215. Grote, K.; Anger, C.; Kelly, B.; Hubbard, S.; Rubin, Y. Characterization of soil water content variability and soil texture using GPR groundwave techniques. *J. Environ. Eng. Geophys.* **2010**, *15*, 93–110. [CrossRef]

216. Zajc, M.; Urbanc, J.; Pečan, U.; Glavan, M.; Pintar, M. Using 3D GPR for determining soil conditions in precision agriculture. In Proceedings of the 18th International Conference Ground Penetrating Radar, Golden, CO, USA, 14–19 November 2020; pp. 291–294. [CrossRef]

217. Koganti, T.; Van De Vijver, E.; Allred, B.J.; Greve, M.H.; Ringgaard, J.; Iversen, B.V. Mapping of agricultural subsurface drainage systems using a frequency-domain ground penetrating radar and evaluating its performance using a single-frequency multi-receiver electromagnetic induction instrument. *Sensors* **2020**, *20*, 3922. [CrossRef]

218. De Benedetto, D.; Castrignano, A.; Sollitto, D.; Modugno, F. Spatial relationship between clay content and geophysical data. *Clay Miner.* **2010**, *45*, 197–207. [CrossRef]

219. Lärm, L.; Bauer, F.; van der Kruk, J.; Vanderborght, J.; Vereecken, H.; Schnepf, A.; Klotzsche, A. Using horizontal borehole GPR data to estimate the effect of maize plants on the spatial and temporal distribution of dielectric permittivity. In Proceedings of the 2021 11th International Workshop on Advanced Ground Penetrating Radar (IWAGPR), Valletta, Malta, 1–4 December 2021; pp. 1–4. [CrossRef]

220. Schneidhofer, P.; Tonning, C.; Cannell, R.J.S.; Nau, E.; Hinterleitner, A.; Verhoeven, G.J.; Gustavsen, L.; Paasche, K.; Neubauer, W.; Gansum, T. The Influence of Environmental Factors on the Quality of GPR Data: The Borre Monitoring Project. *Remote Sens.* **2022**, *14*, 3289. [CrossRef]

221. Igel, J.; Dlugosch, R.; Günther, T.; Müller-Petke, M.; Jiang, C.; Helms, J.; Lang, J.; Winsemann, J. Combined GPR and surface magnetic resonance investigation for aquifer characterisation. In Proceedings of the 2018 17th International Conference on Ground Penetrating Radar (GPR), Rapperswil, Switzerland, 18–21 June 2018; pp. 1–4. [CrossRef]

222. Corwin, D.L.; Lesch, S.M. Apparent soil electrical conductivity measurements in agriculture. *Comput. Electron. Agric.* **2005**, *46*, 11–43. [CrossRef]

223. Van der Kruk, J.; Vereecken, H.; Jacob, R.W. Identifying dispersive GPR signals and inverting for surface wave-guide properties. *Lead. Edge* **2009**, *28*, 1234–1239. [CrossRef]

224. Bradford, J.H. Frequency dependent attenuation of GPR data as a tool for material property characterization: A review and new developments. In Proceedings of the 2011 6th International Workshop on Advanced Ground Penetrating Radar (IWAGPR), Aachen, Germany, 22–24 June 2011; pp. 1–4. [CrossRef]

225. Busch, S.; Van der Kruk, J.; Vereecken, H. Improved characterization of fine-texture soils using on-ground GPR full-waveform inversion. *IEEE Trans. Geosci. Remote Sens.* **2014**, *52*, 3947–3958. [CrossRef]

226. Tosti, F.; Patriarca, C.; Slob, E.; Benedetto, A.; Lambot, S. Clay content evaluation in soils through GPR signal processing. *J. Appl. Geophys.* **2013**, *97*, 69–80. [CrossRef]

227. Benedetto, F.; Tosti, F. GPR spectral analysis for clay content evaluation by the frequency shift method. *J. Appl. Geophys.* **2013**, *97*, 89–96. [CrossRef]

228. Pedrera-Parrilla, A.; Van De Vijver, E.; Van Meirvenne, M.; Espejo-Pérez, A.J.; Giráldez, J.V.; Vanderlinden, K. Apparent electrical conductivity measurements in an olive orchard under wet and dry soil conditions: Significance for clay and soil water content mapping. *Precis. Agric.* **2016**, *17*, 531–545. [CrossRef]

229. Saarenketo, T. Electrical properties of water in clay and silty soils. *J. Appl. Geophys.* **1998**, *40*, 73–88. [CrossRef]

230. Pedret Rodés, J.; Martínez Reguero, A.; Pérez-Gracia, V. GPR spectra for monitoring asphalt pavements. *Remote Sens.* **2020**, *12*, 1749. [CrossRef]

231. Meadows, D.G.; Young, M.H.; McDonald, E.V. Estimating the fine soil fraction of desert pavements using ground penetrating radar. *Vadose Zone J.* **2006**, *5*, 720–730. [CrossRef]

232. Wang, P.; Hu, Z.; Yang, J.; Wang, F.; Gao, M. The identification test of soil texture with ground penetrating radar. In Proceedings of the 2010 International Conference on Advances in Energy Engineering, Beijing, China, 19–20 June 2010; pp. 81–84. [CrossRef]

233. de Mahieu, A.; Ponette, Q.; Mounir, F.; Lambot, S. Using GPR to analyze regeneration success of cork oaks in the Maâmora forest (Morocco). *NDT E Int.* **2020**, *115*, 102297. [CrossRef]

234. Kaufmann, M.S.; Klotzsche, A.; Vereecken, H.; van der Kruk, J. Simultaneous multichannel multi-offset ground-penetrating radar measurements for soil characterization. *Vadose Zone J.* **2020**, *19*, e20017. [CrossRef]

235. Knight, R.; Tercier, P.; Jol, H. The role of ground penetrating radar and geostatistics in reservoir description. *Lead. Edge* **1997**, *16*, 1576–1584. [CrossRef]

236. De Benedetto, D.; Castrignano, A.; Sollitto, D.; Modugno, F.; Buttafuoco, G.; lo Papa, G. Integrating geophysical and geostatistical techniques to map the spatial variation of clay. *Geoderma* **2012**, *171*, 53–63. [CrossRef]

237. De Benedetto, D.; Montemurro, F.; Diacono, M. Mapping an agricultural field experiment by electromagnetic Induction and ground penetrating radar to improve soil water content estimation. *Agronomy* **2019**, *9*, 638. [CrossRef]

238. Bobrov, P.P.; Mironov, V.L.; Kondratyeva, O.V.; Repin, A.V. The effect of clay and organic matter content on the dielectric permittivity of soils and grounds at the frequency range from 10 MHz to 1 GHz. In Proceedings of the 2010 IEEE International Geoscience and Remote Sensing Symposium, Honolulu, HI, USA, 25–30 July 2010; pp. 4433–4435. [CrossRef]

239. Weihermueller, L.; Kaufmann, M.; Steinberger, P.; Pätzold, S.; van der Kruk, J.; Vereecken, H. Fertilization effects on the electrical conductivity measured by EMI, ERT, and GPR. In Proceedings of the EGU General Assembly Conference Abstracts, Vienna, Austria, 8–13 April 2018; p. 4786.

240. Dobson, M.C.; Ulaby, F.T.; Hallikainen, M.T.; El-Rayes, M.A. Microwave dielectric behavior of wet soil-Part II: Dielectric mixing models. *IEEE Trans. Geosci. Remote Sens.* **1985**, *GE-23*, 35–46. [CrossRef]

241. Hudson, B.D. Soil organic matter and available water capacity. *J. Soil Water Conserv.* **1994**, *49*, 189–194.

242. Rawls, W.J.; Pachepsky, Y.A.; Ritchie, J.C.; Sobecki, T.M.; Bloodworth, H. Effect of soil organic carbon on soil water retention. *Geoderma* **2003**, *116*, 61–76. [CrossRef]

243. Jonard, F.; Demontoux, F.; Bircher, S.; Razafindratsima, S.; Schwank, M.; Weillermüller, L.; Lambot, S.; Wigneron, J.P.; Kerr, Y.; Vereecken, H. Electromagnetic characterization of organic-rich soils at the microwave L-band with ground-penetrating radar, radiometry and laboratory measurements. In Proceedings of the 15th International Conference on Ground Penetrating Radar, Brussels, Belgium, 30 June–4 June 2014; pp. 202–207. [CrossRef]

244. Lauer, K.; Albrecht, C.; Salat, C.; Felix-Henningsen, P. Complex effective relative permittivity of soil samples from the taunus region (Germany). *J. Earth Sci.* **2010**, *21*, 961–967. [CrossRef]

245. van Dam, R.L.; van den Berg, E.H.; van Heteren, S.; Kasse, C.; Kenter, J.A.; Groen, K. Influence of organic matter in soils on radar-wave reflection: Sedimentological implications. *J. Sediment. Res.* **2002**, *72*, 341–352. [CrossRef]

246. Wu, Y.; Wang, W.; Zhao, S.; Liu, S. Dielectric properties of saline soils and an improved dielectric model in C-band. *IEEE Trans. Geosci. Remote Sens.* **2014**, *53*, 440–452. [CrossRef]

247. Bircher, S.; Demontoux, F.; Razafindratsima, S.; Zakharova, E.; Drusch, M.; Wigneron, J.-P.; Kerr, Y.H. L-Band Relative Permittivity of Organic Soil Surface Layers—A New Dataset of Resonant Cavity Measurements and Model Evaluation. *Remote Sens.* **2016**, *8*, 1024. [CrossRef]

248. Sarkar, R.; Paul, K.B.; Higgins, T.R. Impacts of Soil Physicochemical Properties and Temporal-Seasonal Soil-Environmental Status on Ground-Penetrating Radar Response. *Soil Sci. Soc. Am. J.* **2019**, *83*, 542–554. [CrossRef]

249. André, F.; Jonard, F.; Jonard, M.; Lambot, S. In situ characterization of forest litter using ground-penetrating radar. *J. Geophys. Res. Biogeosci.* **2016**, *121*, 879–894. [CrossRef]

250. Xiao, L.; Li, C.; Cai, Y.; Zhou, T.; Zhou, M.; Gao, X.; Shi, Y.; Du, H.; Zhou, G.; Zhou, Y. Interactions between soil properties and the rhizome-root distribution in a 12-year Moso bamboo reforested region: Combining ground-penetrating radar and soil coring in the field. *Sci. Total Environ.* **2021**, *800*, 149467. [CrossRef]

251. Williams, R.D.; Ahuja, L.R.; Naney, J.W. Comparison of methods to estimate soil water characteristics from soil texture, bulk density, and limited data. *Soil Sci.* **1992**, *153*, 172–184. [CrossRef]

252. Van Dam, R.L. Calibration functions for estimating soil moisture from GPR dielectric constant measurements. *Commun. Soil Sci. Plant Anal.* **2014**, *45*, 392–413. [CrossRef]

253. Campos, J.R.D.R.; Vidal-Torrado, P.; Modolo, A.J. Use of Ground Penetrating Radar to Study Spatial Variability and Soil Stratigraphy. *Eng. Agríc.* **2019**, *39*, 358–364. [CrossRef]

254. Szypłowska, A.; Lewandowski, A.; Yagihara, S.; Saito, H.; Furuhata, K.; Szerement, J.; Kafarski, M.; Wilczek, A.; Majcher, J.; Woszczyk, A.; et al. Dielectric models for moisture determination of soils with variable organic matter content. *Geoderma* **2021**, *401*, 115288. [CrossRef]

255. Jin, M.; Zheng, X.; Jiang, T.; Li, X.; Li, X.-J.; Zhao, K. Evaluation and improvement of SMOS and SMAP soil moisture products for soils with high organic matter over a forested area in Northeast China. *Remote Sens.* **2017**, *9*, 387. [CrossRef]

256. Park, C.H.; Berg, A.; Cosh, M.H.; Colliander, A.; Behrendt, A.; Manns, H.; Hong, J.; Lee, J.; Zhang, R.; Wulfmeyer, V. An inverse dielectric mixing model at 50 MHz that considers soil organic carbon. *Hydrol. Earth Syst. Sci.* **2021**, *25*, 6407–6420. [CrossRef]

257. Ikazaki, K.; Nagumo, F.; Simporé, S.; Barro, A. Soil toposequence, productivity, and a simple technique to detect petroplinthites using ground-penetrating radar in the Sudan Savanna. *Soil Sci. Plant Nutr.* **2018**, *64*, 623–631. [CrossRef]

258. Idi, B.Y. Application of Ground Penetrating Radar for Spatial Mapping of Organic Contents in Potian Peat Soil, Johor Malaysia. *Dutse J. Pure Appl. Sci.* **2019**, *5*, 31–38.

259. Li, L.; Xia, Y.H.; Liu, S.J.; Zhang, W.; Chen, X.B.; Zheng, H.; Qiu, H.S.; He, X.Y.; Su, Y.R. Modified method for estimating organic carbon density in discontinuous Karst soil using ground-penetrating radar and geostatistics. *J. Mt. Sci.* **2015**, *12*, 1229–1240. [CrossRef]

260. Winkelbauer, J.; Völkel, J.; Leopold, M.; Bernt, N. Methods of surveying the thickness of humous horizons using ground penetrating radar (GPR): An example from the Garmisch-Partenkirchen area of the Northern Alps. *Eur. J. For. Res.* **2011**, *130*, 799–812. [CrossRef]

261. Zajícová, K.; Chuman, T. O and A soil horizons' boundaries detection using GPR under variable soil moisture conditions. *Geoderma* **2022**, *422*, 115934. [CrossRef]

262. Alaoui, A.; Diserens, E. Mapping soil compaction—A review. *Curr. Opin. Environ. Sci. Health* **2018**, *5*, 60–66. [CrossRef]

263. Hanxiao, X.; Yingui, C.; Gubai, L.; Shufeti, W.; Jinman, W.; Zhongke, B. Variability in reconstructed soil bulk density of a high moisture content soil: A study on feature identification and ground penetrating radar detection. *Environ. Earth Sci.* **2022**, *81*, 249. [CrossRef]

264. Akinsunmade, A.; Tomecka-Suchoń, S.; Pysz, P. Correlation between agrotechnical properties of selected soil types and corresponding GPR response. *Acta Geophys.* **2019**, *67*, 1913–1919. [CrossRef]

265. Gong, Y.; Cao, Q.; Sun, Z. The effects of soil bulk density, clay content and temperature on soil water content measurement using time-domain reflectometry. *Hydrol. Process.* **2003**, *17*, 3601–3614. [CrossRef]

266. Perdok, U.D.; Kroesbergen, B.; Hilhorst, M.A. Influence of gravimetric water content and bulk density on the dielectric properties of soil. *Eur. J. Soil Sci.* **1996**, *47*, 367–371. [CrossRef]

267. Malicki, M.A.; Campbell, E.C.; Hanks, R.J. Investigations on power factor of the soil electrical impedance as related to moisture, salinity and bulk density. *Irrig. Sci.* **1989**, *10*, 55–62. [CrossRef]

268. Petersen, H.; Rabbel, W.; Horn, R.; Volk, L. Sensitivity of Electrical Properties to Soil Compaction-Case Study. In Proceedings of the Near Surface 2010-16th EAGE European Meeting of Environmental and Engineering Geophysics, Houten, The Netherlands, 6–8 September 2010; p. cp-164. [CrossRef]

269. Lombardi, F.; Lualdi, M. Step—Frequency Ground Penetrating Radar for agricultural soil morphology characterisation. *Remote Sens.* **2019**, *11*, 1075. [CrossRef]

270. Wang, P.; Hu, Z.; Zhao, Y.; Li, X. Experimental study of soil compaction effects on GPR signals. *J. Appl. Geophys.* **2016**, *126*, 128–137. [CrossRef]

271. Akinsunmade, A.; Tomecka-Suchoń, S.; Kiełbasa, P.; Juliszewski, T.; Pysz, P.; Karczewski, J.; Zagórda, M. GPR geophysical method as a remediation tool to determine zones of high penetration resistance of soil. *J. Phys. Conf. Ser.* **2021**, *1782*, 012001. [CrossRef]

272. De-Ville, S.; Pattison, I.; Frost, M. COMPACT: A frequency analysis of Ground Penetrating Radar to identify agricultural soil compaction. In Proceedings of the AGU Fall Meeting Abstracts, Washington, DC, USA, 10–14 December 2018; Volume 2018, p. NS13B-0596.

273. De-Ville, S.; Pattison, I.; Frost, M.; Demirci, E. Taking novel approaches of Ground Penetrating Radar and Computed Tomography to quantify the location and severity of soil compaction in agricultural landscapes. In Proceedings of the Geophysical Research Abstracts, Vienna, Austria, 10 January 2019; Volume 21.

274. Akinniyi, A.; Jerzy, K.; Paweł, P.; Sylwia, T.S.; Tadeusz, U. Identification of heavy machines impact on soil using Ground Penetrating Radar. In *Advances in Mechanism and Machine Science. IFToMM WC 2019*; Mechanisms and Machine Science; Uhl, T., Ed.; Springer: Cham, Switzerland, 2019; Volume 73. [CrossRef]

275. Petersen, H.; Fleige, H.; Rabbel, W.; Horn, R. Applicability of geophysical prospecting methods for mapping of soil compaction and variability of soil texture on farm land. *J. Plant Nutr. Soil Sci.-Z. Pflanzenernahr. Bodenkd.* **2005**, *168*, 68–79. [CrossRef]

276. Muñiz, E.; Shaw, R.K.; Gimenez, D.; Williams, C.A.; Kenny, L. Use of Ground-Penetrating Radar to Determine Depth to Compacted Layer in Soils Under Pasture. In *Digital Soil Morphometrics. Progress in Soil Science*; Hartemink, A., Minasny, B., Eds.; Springer: Cham, Switzerland, 2016. [CrossRef]

277. Afshar, F.A.; Ayoubi, S.; Castrignanò, A.; Quarto, R.; Ardekani, M.R.M. Using ground-penetrating radar to explore the cemented soil horizon in an arid region in Iran. *Near Surf. Geophys.* **2017**, *15*, 103–110. [CrossRef]

278. Keller, T.; Colombi, T.; Ruiz, S.; Manalili, M.P.; Rek, J.; Stadelmann, V.; Wunderli, H.; Breitenstein, D.; Reiser, R.; Oberholzer, H.; et al. Long-term Soil Structure Observatory for monitoring post-compaction evolution of soil structure. *Vadose Zone J.* **2017**, *16*, 118. [CrossRef]

279. Cui, F.; Wu, Z.Y.; Wang, L.; Wu, Y.B. Application of the Ground Penetrating Radar ARMA power spectrum estimation method to detect moisture content and compactness values in sandy loam. *J. Appl. Geophys.* **2015**, *120*, 26–35. [CrossRef]

280. Iwasaki, K.; Tamura, M.; Sato, H.; Masaka, K.; Oka, D.; Yamakawa, Y.; Kosugi, K. Application of Ground-Penetrating Radar and a Combined Penetrometer–Moisture Probe for Evaluating Spatial Distribution of Soil Moisture and Soil Hardness in Coastal and Inland Windbreaks. *Geosciences* **2020**, *10*, 238. [CrossRef]

281. Kiełbasa, P.; Zagórda, M.; Juliszewski, T.; Akinsunmade, A.; Tomecka, S.; Karczewski, J.; Pysz, P. Assessment of the possibility of using GPR to determine the working resistance force of tools for subsoil reclamation. *J. Phys. Conf. Ser.* **2021**, *1782*, 012013. [CrossRef]

282. Keller, T.; Lamandé, M.; Naderi-Boldaji, M.; de Lima, R.P. Soil Compaction Due to Agricultural Field Traffic: An Overview of Current Knowledge and Techniques for Compaction Quantification and Mapping. In *Advances in Understanding Soil Degradation. Innovations in Landscape Research*; Saljnikov, E., Mueller, L., Lavrishchev, A., Eulenstein, F., Eds.; Springer: Cham, Switzerland, 2022. [CrossRef]

283. Akinsunmade, A. GPR imaging of traffic compaction effects on soil structures. *Acta Geophys.* **2021**, *69*, 643–653. [CrossRef]

284. Mount, G.J.; Comas, X. Estimating porosity and solid dielectric permittivity in the Miami Limestone using high-frequency ground penetrating radar (GPR) measurements at the laboratory scale. *Water Resour. Res.* **2014**, *50*, 7590–7605. [CrossRef]

285. Bradford, J.H.; Clement, W.P.; Barrash, W. Estimating porosity with ground-penetrating radar reflection tomography: A controlled 3-D experiment at the Boise Hydrogeophysical Research Site. *Water Resour. Res.* **2009**, *45*, W00D26. [CrossRef]

286. Ghose, R.; Slob, E.C. Quantitative integration of seismic and GPR reflections to derive unique estimates for water saturation and porosity in subsoil. *Geophys. Res. Lett.* **2006**, *33*, L05404. [CrossRef]

287. Clement, W.P.; Knoll, M.D. Traveltime inversion of vertical radar profiles. *Geophysics* **2006**, *71*, K67–K76. [CrossRef]

288. Roodposhti, H.R.; Hafizi, M.K.; Kermani, M.R.S. Ground Penetrating Radar for water content and compaction evaluation: A laboratory test on construction material. *J. Environ. Eng. Geophys.* **2020**, *25*, 169–179. [CrossRef]

289. Turesson, A. Water content and porosity estimated from ground-penetrating radar and resistivity. *J. Appl. Geophys.* **2006**, *58*, 99–111. [CrossRef]

290. Cunningham, K.J. Application of ground-penetrating radar, digital optical borehole images, and cores for characterization of porosity hydraulic conductivity and paleokarst in the Biscayne aquifer, southeastern Florida, USA. *J. Appl. Geophys.* **2004**, *55*, 61–76. [CrossRef]

291. Causse, E.; Sénéchal, P. Model-based automatic dense velocity analysis of GPR field data for the estimation of soil properties. *J. Geophys. Eng.* **2006**, *3*, 169–176. [CrossRef]

292. Mount, G.J.; Comas, X.; Wright, W.J.; McClellan, M.D. Delineation of macroporous zones in the unsaturated portion of the Miami Limestone using ground penetrating radar, Miami Dade County, Florida. *J. Hydrol.* **2015**, *527*, 872–883. [CrossRef]

293. Kaufmann, M.S.; Klotzsche, A.; Dal Bo, I.; Vereecken, H.; Van Der Kruk, J. Determining large scale soil permittivity with simultaneous multi-channel GPR measurement. In Proceedings of the AGU Fall Meeting Abstracts, Washington, DC, USA, 10–14 December 2018; Volume 2018, p. NS13B-0597.

294. Harbi, H.; McMechan, G.A. Modeling 3D porosity and permeability from GPR data in the Ellenburger Dolomite, central Texas. *Geophysics* **2011**, *76*, J35–J46. [CrossRef]

295. Lassen, R.N.; Sonnenborg, T.O.; Jensen, K.H.; Looms, M.C. Monitoring CO_2 gas-phase migration in a shallow sand aquifer using cross-borehole ground penetrating radar. *Int. J. Greenh. Gas Control* **2015**, *37*, 287–298. [CrossRef]

296. Nielsen, L.; Looms, M.C.; Hansen, T.M.; Cordua, K.S.; Stemmerik, L. Estimation of chalk heterogeneity from stochastic modeling conditioned by crosshole GPR traveltimes and log data. *Adv. Near-Surf. Seismol. Ground-Penetrating Radar SEG Geophys. Dev. Ser.* **2010**, *15*, 379–398. [CrossRef]

297. Lu, D.; Wang, H.; Geng, N.; Xia, Y.; Xu, C.; Hua, E. Imaging and characterization of the preferential flow process in agricultural land by using electrical resistivity tomography and dual-porosity model. *Ecol. Indic.* **2022**, *134*, 108498. [CrossRef]

298. Keskinen, J.; Klotzsche, A.; Looms, M.C.; Moreau, J.; van der Kruk, J.; Holliger, K.; Stemmerik, L.; Nielsen, L. Full-waveform inversion of crosshole GPR data: Implications for porosity estimation in chalk. *J. Appl. Geophys.* **2017**, *140*, 102–116. [CrossRef]

299. Klotzsche, A.; van der Kruk, J.; Bradford, J.; Vereecken, H. Detection of spatially limited high-porosity layers using crosshole GPR signal analysis and full-waveform inversion. *Water Resour. Res.* **2014**, *50*, 6966–6985. [CrossRef]

300. van der Kruk, J.; Gueting, N.; Klotzsche, A.; He, G.; Rudolph, S.; von Hebel, C.; Yang, X.; Weihermüller, L.; Mester, A.; Vereecken, H. Quantitative multi-layer electromagnetic induction inversion and full-waveform inversion of crosshole ground penetrating radar data. *J. Earth Sci.* **2015**, *26*, 844–850. [CrossRef]

301. Finsterle, S.; Kowalsky, M.B. Joint hydrological–geophysical inversion for soil structure identification. *Vadose Zone J.* **2008**, *7*, 287–293. [CrossRef]

302. Liu, T.; Su, Y.; Huang, C. Inversion of ground penetrating radar data based on neural networks. *Remote Sens.* **2018**, *10*, 730. [CrossRef]

303. Kotlar, A.M.; Iversen, B.V.; de Jong van Lier, Q. Evaluation of parametric and nonparametric machine-learning techniques for prediction of saturated and near-saturated hydraulic conductivity. *Vadose Zone J.* **2019**, *18*, 1–13. [CrossRef]

304. Walker, J.P.; Willgoose, G.R.; Kalma, J.D. One-dimensional soil moisture profile retrieval by assimilation of near-surface measurements: A simplified soil moisture model and field application. *J. Hydrometeorol.* **2001**, *2*, 356–373. [CrossRef]

305. Léger, E.; Saintenoy, A.; Coquet, Y. Hydrodynamic parameters of a sandy soil determined by ground-penetrating radar inside a single ring infiltrometer. *Water Resour. Res.* **2014**, *50*, 5459–5474. [CrossRef]

306. de Jong, S.M.; Heijenk, R.A.; Nijland, W.; van der Meijde, M. Monitoring soil moisture dynamics using electrical resistivity tomography under homogeneous field conditions. *Sensors* **2020**, *20*, 5313. [CrossRef]

307. Moua, R.; Lesparre, N.; Girard, J.F.; Belfort, B.; Lehmann, F. Estimate of hydrodynamic parameters with a coupled hydrogeophysical inversion using GPR surveys. In Proceedings of the EGU General Assembly Conference Abstracts, Virtual, 19–30 April 2021; p. EGU21-8705.

308. Xiao, X.; Guan, B.; Ihamouten, A.; Villain, G.; Dérobert, X.; Tian, G. Monitoring water transfers in limestone building materials with water retention curve and Ground Penetrating Radar: A comparative study. *NDT E Int.* **2018**, *100*, 31–39. [CrossRef]

309. Luo, G.; Cao, Y.; Xu, H.; Yang, G.; Wang, S.; Huang, Y.; Bai, Z. Detection of soil physical properties of reclaimed land in open-pit mining area: Feasibility of application of ground penetrating radar. *Environ. Monit. Assess.* **2021**, *193*, 392. [CrossRef]

310. Grote, K.; Leverett, K. Comparison of pedotransfer functions for high-resolution mapping of hydraulic conductivity in agricultural soils using GPR. In Proceedings of the AGU Fall Meeting Abstracts, San Francisco, CA, USA, 9–13 December 2019; Volume 2019, p. NS31A-0762.

311. Gloaguen, E.; Chouteau, M.; Marcotte, D.; Chapuis, R. Estimation of hydraulic conductivity of an unconfined aquifer using cokriging of GPR and hydrostratigraphic data. *J. Appl. Geophys.* **2001**, *47*, 135–152. [CrossRef]

312. Schmalz, B.; Lennartz, B. Analyses of soil water content variations and GPR attribute distributions. *J. Hydrol.* **2002**, *267*, 217–226. [CrossRef]

313. Brooks, R.H.; Corey, A.T. Properties of porous media affecting fluid flow. *J. Irrig. Drain. Div.* **1966**, *92*, 61–88. [CrossRef]

314. Kosugi, K.I. Lognormal distribution model for unsaturated soil hydraulic properties. *Water Resour. Res.* **1996**, *32*, 2697–2703. [CrossRef]

315. Oikawa, K.; Kuroda, S.; Saito, H. Velocity analysis of time-lapse sparse array antenna GPR CMP data to estimate infiltration front depth: A numerical study. In Proceedings of the AGU Fall Meeting Abstracts, Chicago, IL, USA, 12–16 December 2020; Volume 2020, p. H003-13.

316. Klenk, P.; Jaumann, S.; Roth, K. Quantitative high-resolution observations of soil water dynamics in a complicated architecture using time-lapse ground-penetrating radar. *Hydrol. Earth Syst. Sci.* **2015**, *19*, 1125–1139. [CrossRef]

317. Chen, J.; Hubbard, S.; Rubin, Y. Estimating the hydraulic conductivity at the South Oyster Site from geophysical tomographic data using Bayesian techniques based on the normal linear regression model. *Water Resour. Res.* **2001**, *37*, 1603–1613. [CrossRef]

318. Di Prima, S.; Giannini, V.; Ribeiro Roder, L.; Stewart, R.D.; Abou Najm, M.R.; Longo, V.; Winiarski, T.; Angulo-Jaramillo, R.; Pirastru, M.; Lassabatere, L.; et al. Using GPR surveys and infiltration experiments for assessing soil physical quality of an agricultural soil. In Proceedings of the EGU General Assembly Conference Abstracts, Virtual, 19–30 April 2021; p. EGU21-2034.

319. Weihnacht, B.; Boerner, F. Measurement of retention functions with hysteresis using ground-penetrating radar. *Near Surf. Geophys.* **2014**, *12*, 539–548. [CrossRef]

320. Saintenoy, A.; Schneider, S.; Tucholka, P. Evaluating ground penetrating radar use for water infiltration monitoring. *Vadose Zone J.* **2008**, *7*, 208–214. [CrossRef]

321. Köpke, C.; Irving, J.; Roubinet, D. Stochastic inversion for soil hydraulic parameters in the presence of model error: An example involving ground-penetrating radar monitoring of infiltration. *J. Hydrol.* **2019**, *569*, 829–843. [CrossRef]

322. Shakas, A.; Maurer, H.; Giertzuch, P.L.; Hertrich, M.; Giardini, D.; Serbeto, F.; Meier, P. Permeability enhancement from a hydraulic stimulation imaged with Ground Penetrating Radar. *Geophys. Res. Lett.* **2020**, *47*, e2020GL088783. [CrossRef]

323. Leger, E.; Saintenoy, A.C.; Coquet, Y. Soil water retention function hysteresis determined by ground-penetrating radar. In Proceedings of the AGU Fall Meeting Abstracts, San Francisco, CA, USA, 15–19 December 2014; Volume 2014, p. NS21B-3882.

324. Angulo-Jaramillo, R.; Vandervaere, J.P.; Roulier, S.; Thony, J.L.; Gaudet, J.P.; Vauclin, M. Field measurement of soil surface hydraulic properties by disc and ring infiltrometers: A review and recent developments. *Soil Tillage Res.* **2000**, *55*, 1–29. [CrossRef]

325. Léger, E.; Saintenoy, A.; Coquet, Y. Estimating saturated hydraulic conductivity from ground-based GPR monitoring Porchet infiltration in sandy soil. In Proceedings of the 15th International Conference on Ground Penetrating Radar, Brussels, Belgium, 30 June–4 June 2014; pp. 124–130. [CrossRef]

326. Léger, E.; Saintenoy, A.; Coquet, Y.; Tucholka, P.; Zeyen, H. Evaluating hydrodynamic parameters accounting for water retention hysteresis in a large sand column using surface GPR. *J. Appl. Geophys.* **2020**, *182*, 104176. [CrossRef]

327. Tran, A.P.; Vanclooster, M.; Zupanski, M.; Lambot, S. Joint estimation of soil moisture profile and hydraulic parameters by ground-penetrating radar data assimilation with maximum likelihood ensemble filter. *Water Resour. Res.* **2014**, *50*, 3131–3146. [CrossRef]

328. Dagenbach, A.; Buchner, J.S.; Klenk, P.; Roth, K. Identifying a parameterisation of the soil water retention curve from on-ground GPR measurements. *Hydrol. Earth Syst. Sci.* **2013**, *17*, 611–618. [CrossRef]

329. Bano, M. Effects of the transition zone above a water table on the reflection of GPR waves. *Geophys. Res. Lett.* **2006**, *33*, L13309. [CrossRef]

330. Saintenoy, A.; Hopmans, J.W. Ground penetrating radar: Water table detection sensitivity to soil water retention properties. *IEEE J. Sel. Top. Appl. Earth Obs. Remote Sens.* **2011**, *4*, 748–753. [CrossRef]

331. Guellouz, L.; Askri, B.; Jaffré, J.; Bouhlila, R. Estimation of the soil hydraulic properties from field data by solving an inverse problem. *Sci. Rep.* **2020**, *10*, 9359. [CrossRef] [PubMed]

332. Léger, E.; Saintenoy, A.; Tucholka, P.; Coquet, Y. Inverting surface GPR data to estimate wetting and drainage water retention curves in laboratory. In Proceedings of the 2015 8th International Workshop on Advanced Ground Penetrating Radar (IWAGPR), Florence, Italy, 7–10 July 2015; pp. 1–5. [CrossRef]

333. Lambot, S.; Antoine, M.; Van den Bosch, I.; Slob, E.C.; Vanclooster, M. Electromagnetic inversion of GPR signals and subsequent hydrodynamic inversion to estimate effective vadose zone hydraulic properties. *Vadose Zone J.* **2004**, *3*, 1072–1081. [CrossRef]

334. Tran, A.P.; Ardekani, M.R.M.; Lambot, S. Coupling of dielectric mixing models with full-wave ground-penetrating radar signal inversion for sandy-soil-moisture estimation. *Geophysics* **2012**, *77*, H33–H44. [CrossRef]

335. Minet, J.; Wahyudi, A.; Bogaert, P.; Vanclooster, M.; Lambot, S. Mapping shallow soil moisture profiles at the field scale using full-waveform inversion of ground penetrating radar data. *Geoderma* **2011**, *161*, 225–237. [CrossRef]

336. Jadoon, K.Z.; Weihermuller, L.; Scharnagl, B.; Kowalsky, M.B.; Bechtold, M.; Hubbard, S.S.; Vereecken, H.; Lambot, S. Estimation of soil hydraulic parameters in the field by integrated hydrogeophysical inversion of time-lapse ground-penetrating radar data. *Vadose Zone J.* **2012**, *11*, vzj2011.0177. [CrossRef]

337. Köpke, C.; Irving, J.; Elsheikh, A.H. Accounting for model error in Bayesian solutions to hydrogeophysical inverse problems using a local basis approach. *Adv. Water Resour.* **2018**, *116*, 195–207. [CrossRef]

338. Yu, Y.; Huisman, J.A.; Klotzsche, A.; Vereecken, H.; Weihermüller, L. Coupled full-waveform inversion of horizontal borehole ground penetrating radar data to estimate soil hydraulic parameters: A synthetic study. *J. Hydrol.* **2022**, *610*, 127817. [CrossRef]

339. Oikawa, K.; Saito, H.; Kuroda, S. Effect of soil type on estimating infiltration front depth and hydraulic conductivity using time-lapse array antenna GPR multi-offset gather: A numerical study. In Proceedings of the 18th International Conference on Ground Penetrating Radar, Golden, CO, USA, 18–21 November 2020; pp. 303–306. [CrossRef]

340. Evett, S.R.; Parkin, G.W. Advances in soil water content sensing: The continuing maturation of technology and theory. *Vadose Zone J.* **2005**, *4*, 986–991. [CrossRef]

341. Vereecken, H.; Huisman, J.A.; Bogena, H.; Vanderborght, J.; Vrugt, J.A.; Hopmans, J.W. On the value of soil moisture measurements in vadose zone hydrology: A review. *Water Resour. Res.* **2008**, *44*, W00D06. [CrossRef]

342. Robertson, B.B.; Almond, P.C.; Carrick, S.T.; Penny, V.; Chau, H.W.; Smith, C.M. Variation in matric potential at field capacity in stony soils of fluvial and alluvial fans. *Geoderma* **2021**, *392*, 114978. [CrossRef]

343. Sreelash, K.; Buis, S.; Sekhar, M.; Ruiz, L.; Tomer, S.K.; Guerif, M. Estimation of available water capacity components of two-layered soils using crop model inversion: Effect of crop type and water regime. *J. Hydrol.* **2017**, *546*, 166–178. [CrossRef]

344. Nourbakhsh, F.; Afyuni, M.; Abbaspour, K.C.; Schulin, R. Research note: Estimation of field capacity and wilting point from basic soil physical and chemical properties. *Arid. Land Res. Manag.* **2004**, *19*, 81–85. [CrossRef]

345. Galagedara, L.W.; Redman, J.D.; Parkin, G.W.; Annan, A.P.; Endres, A.L. Numerical modeling of GPR to determine the direct ground wave sampling depth. *Vadose Zone J.* **2005**, *4*, 1096–1106. [CrossRef]

346. Park, C.-H.; Montzka, C.; Jagdhuber, T.; Jonard, F.; De Lannoy, G.; Hong, J.; Jackson, T.J.; Wulfmeyer, V. A Dielectric Mixing Model Accounting for Soil Organic Matter. *Vadose Zone J.* **2019**, *18*, 190036. [CrossRef]

347. Wang, R.; Gao, P.; Zhou, E.; Li, Y.; Zhao, G. Experimental detection of the volume of the drip irrigation soil wetted body using Ground Penetrating Radar. *J. Soil Water Conserv.* **2021**, *76*, 199–210. [CrossRef]

348. Harmsen, E.; Parsiani, H.; Torres, M. Evaluation of several dielectric mixing models for estimating soil moisture content in sand, loam and clay soils. In Proceedings of the 2003 ASAE Annual Meeting, Las Vegas, NV, USA, 27–30 July 2003; p. 1. [CrossRef]